Oligonucleotide Analogues with Integrated Bases and Backbone

Part 15[1])

Synthesis and Association of Ethenylene-Linked Self-Complementary Dimers

by **Xiaomin Zhang**, **Bruno Bernet**, and **Andrea Vasella***

Laboratorium für Organische Chemie, ETH Zürich, Wolfgang-Pauli-Strasse 10, CH-8093 Zürich
(e-mail: vasella@org.chem.ethz.ch)

The self-complementary (*Z*)-configured U*[c_e]A$^{(*)}$ dinucleotide analogues **6**, **8**, **10**, **12**, **14**, and **16**, and the A*[c_e]U$^{(*)}$ dimers **19**, **21**, **23**, **25**, **27**, and **29** were prepared by partial hydrogenation of the corresponding ethynylene linked dimers. Photolysis of **14** led to the (*E*)-alkene **17**. These dinucleotide analogues associate in $CDCl_3$ solution, as evidenced by NMR and CD spectroscopy. The thermodynamic parameters of the duplexation were determined by *van't Hoff* analysis. The (*Z*)-configured U*[c_e]A$^{(*)}$ dimers **14** and **16** form cyclic duplexes connected by *Watson–Crick* H-bonds, the (*E*)-configured U*[c_e]A dimer **17** forms linear duplexes, and the U*[c_e]A$^{(*)}$ allyl alcohols **6**, **8**, **10**, and **12** form mixtures of linear and cyclic duplexes. The *C*(6/I)-unsubstituted A*[c_e]U allyl alcohols **19** and **23** form linear duplexes, whereas the *C*(6/I)-substituted A*[c_e]U* allyl alcohols **21** and **25**, and the *C*(5′/I)-deoxy A*[c_e]U$^{(*)}$ dimers **27** and **29** also form minor amounts of cyclic duplexes. The influence of intra- and intermolecular H-bonding of the allyl alcohols and the influence of the base sequence upon the formation of cyclic duplexes are discussed.

Introduction. – We have analyzed the association of self-complementary ethynylene-linked di- and tetranucleotide analogues where the ethynylene linker replaces the contiguous backbone of oligonucleotides, resulting in oligonucleosides with integrated bases and backbone (ONIBs) [1][2]. Their association to form cyclic duplexes requires a *syn*-conformation of the nucleobase (unit I in **1**–**4**) and a *gg*-type conformation of the ethynyl at C(5′/I). The ethynylene linker of **1** and **2** orients its substituents in a rigid, well-defined way, raising the question about the extent to which the specific orientation and its rigidity are prerequisites for the formation of cyclic duplexes. We wondered if a different, but also well-defined orientation of the substituents of a C_2-linker between nucleobase and C(5″/I) of self-complementary dimers, as in the conformationally restricted (*Z*)-analogues **3** and **4** and their (*E*)-isomers is compatible with the formation of cyclic duplexes. The dimeric U*[c_y]A$^{(*)}$ [2]) propargylic alcohols **1** (X = OH) are characterized by a strongly persistent intramolecular H-bond of HO–C(5′/I) to N(3/I). It imposes a *gg*- or *tg*-orientation of the ethynyl moiety, and prevents the

[1]) Part 14: [1].

[2]) *Conventions for abbreviated notation:* The substitution at C(6) of pyrimidines and C(8) of purines is denoted by an asterisk (*); for example U* and A* for methylated uridine and adenosine derivatives. U$^{(*)}$ and A$^{(*)}$ represents both unsubstituted and methylated nucleobases. The moiety linking C(6)CH_2 or C(8)CH_2, and C(5′) of the previous unit is indicated in square brackets, such as [c] for a C-atom. The indices y, e, and a indicate a triple, double, or single bond, respectively.

formation of cyclic duplexes so that these propargylic alcohols can only form linear duplexes and higher associates. The propargylic HO–C(5′/I) group of the A*[c_y]U$^{(*)}$ dimers **2** (X = OH), however, forms only a weakly persistent intramolecular H-bond to O=C(2/I) of the uracil moiety, and may even form an intermolecular H-bond in cyclic duplexes. Conceivably, the allylic OH group in the U*[c_e]A$^{(*)}$ and A*[c_e]U$^{(*)}$ dimers **3** and **4** (X = OH) will play a similar role, suggesting to synthesize both the allylic alcohols and their *C*(5′)-deoxy analogues.

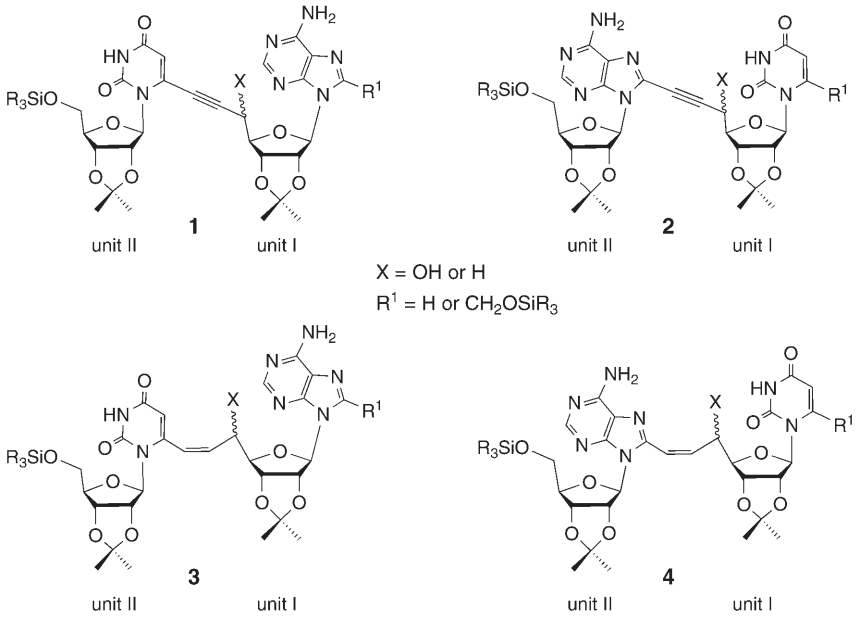

The (*Z*)-alkenes **3** and **4** (X = OH or H) should be easily accessible by partial reduction of **1** and **2**, respectively. We report on the synthesis of these alkenes and one of their (*E*)-isomers, and detail the analysis of their association.

Results and Discussion. – 1. *Synthesis.* Partial hydrogenation of the U*[c_y]A$^{(*)}$ acetylenes **7**, **9**, **11**, **13**, and **15** [2] in the presence of a *Lindlar* catalyst gave the desired (*Z*)-alkenes **8**, **10**, **12**, **14**, and **16**, respectively (*Scheme 1*). There was no obvious influence of the propargylic OH group on the ease of hydrogenation. Hydrogenation of **5** to the (*Z*)-alkene **6** was incomplete, even in the presence of a larger amount of *Lindlar* catalyst and under 5.5 bar of H_2, while hydrogenation in the presence of 10% Pd/C under 5 bar of H_2 gave **6** in a yield of 57%. The high yield of **8**, **10**, and **14** (92–94%), the lower yield of **12** and **16** (76%), and the reduced reactivity of **5** are not readily rationalized. Photolysis transformed **14** in 88% yield into the (*E*)-alkene **17**.

The A*[c_y]U$^{(*)}$ alkynes (*Scheme 2*) proved far more reactive towards *Lindlar* hydrogenation than the U*[c_y]A$^{(*)}$ isomers. Partial over-reduction could not be avoided even by diminishing the amount of catalyst. The reaction conditions (solvent,

Scheme 1

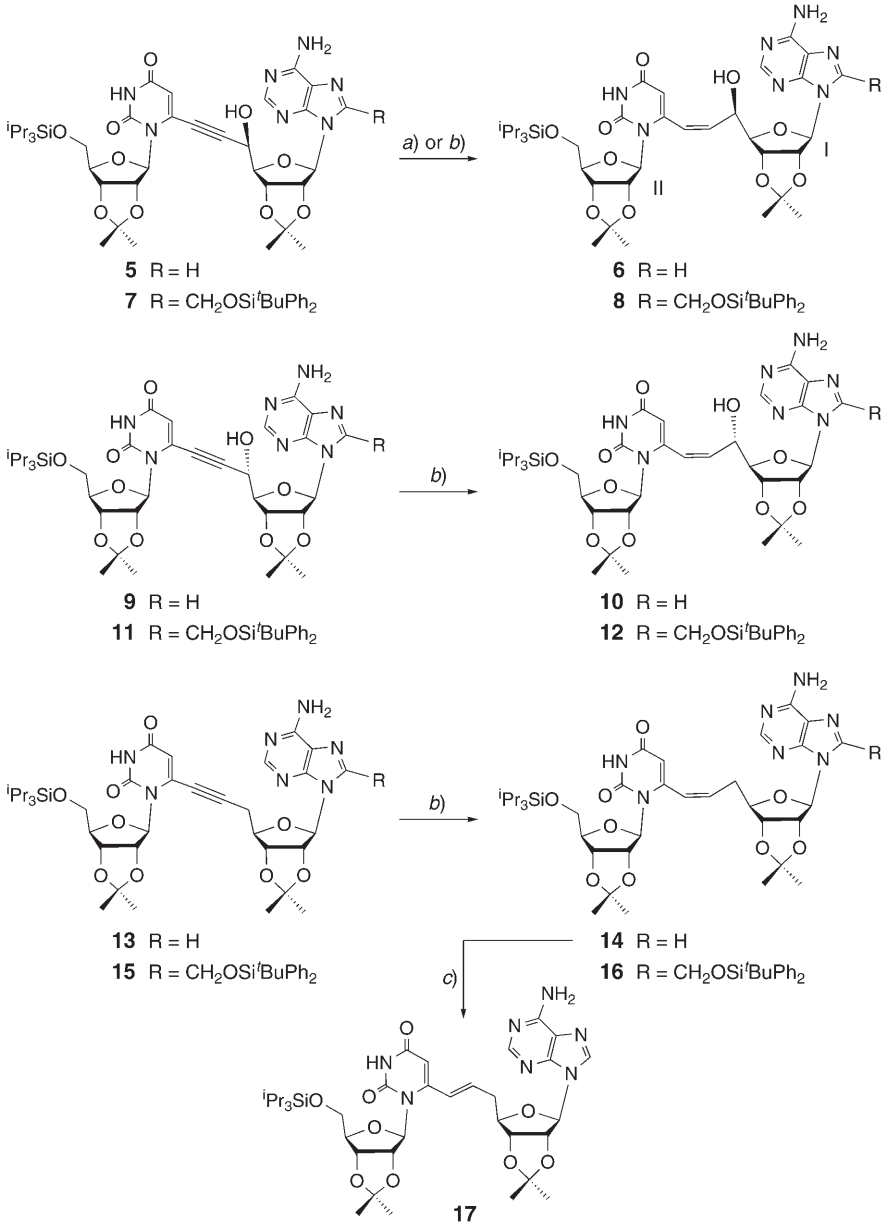

a) 10% Pd/C, 5 bar of H_2, MeOH; 57% of **6**. *b*) 5% Pd/$BaSO_4$, quinoline, 1 bar of H_2, MeOH; 92% of **8**; 94% of **10**; 76% of **12**; 92% of **14**; 76% of **16**. *c*) I_2, *hν* (Hg lamp), toluene; 88%.

Scheme 2

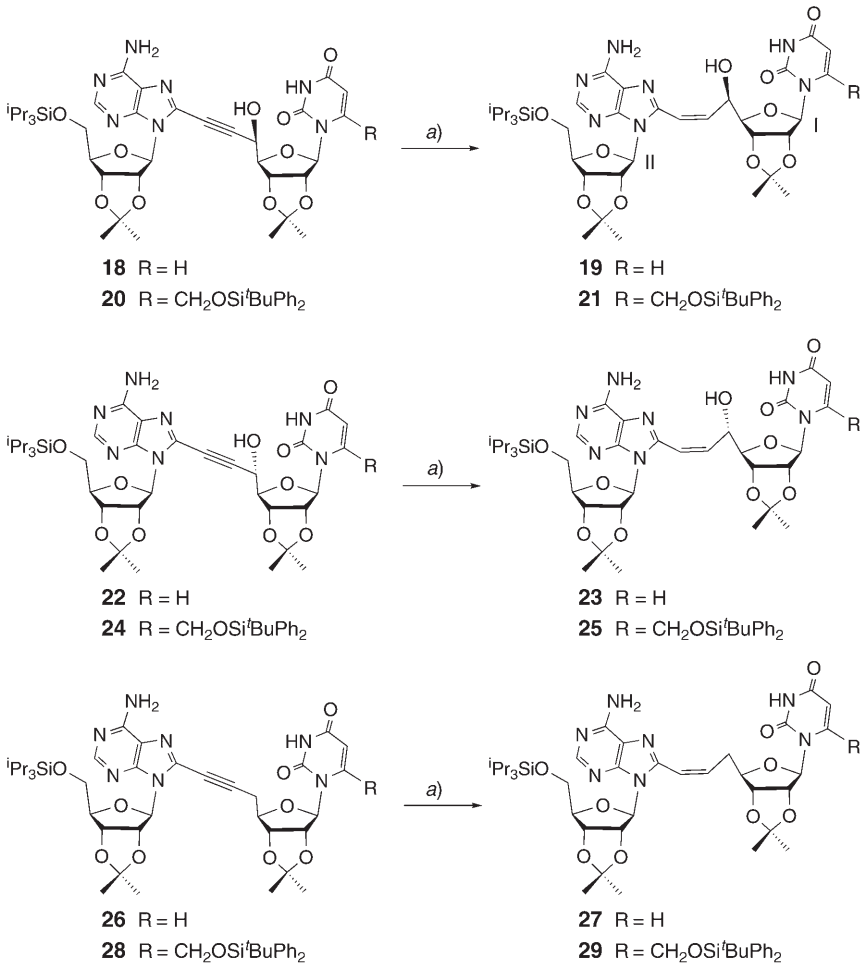

a) 5% Pd/$BaSO_4$, quinoline, 1 bar of H_2, MeOH; 47% of **19**; 78% of **21**; 71% of **23**; 74% of **25**; 70% of **27**; 48% of **29**.

amount of catalyst, amount of quinoline, H_2 pressure, and reaction time) were optimized for the *Lindlar* hydrogenation of the deoxygenated alkyne **26**. Best conditions involved hydrogenation in MeOH under 1 bar of H_2 to provide 70% of **27**. Similarly, the propargylic alcohols **20**, **22**, and **24** were transformed in 71–78% yield into the desired (*Z*)-alkenes **21**, **23**, and **25**, respectively. Lower yields of **19** and **29** (47–48%) resulted from hydrogenation of **18** and **28** under the same conditions.

2. *Association of the U*[c$_e$]A$^{(*)}$ and A*[c$_e$]U$^{(*)}$ Dimers in CHCl$_3$ Solution*. Solutions of the U*[c$_e$]A$^{(*)}$ and A*[c$_e$]U$^{(*)}$ dinucleosides in $CHCl_3$ were expected to associate, forming linear duplexes and higher associates and/or cyclic duplexes, similarly as the

U*[c_y]A$^{(*)}$ and A*[c_y]U$^{(*)}$ dinucleosides [2]. The ability of these ethynylene-linked dinucleosides to form cyclic duplexes depends mainly on the following structural parameters of unit I: *1*) the orientation of the nucleobase, as specified by the χ angle and depending on the presence of a substituent at C(6) of U or C(8) of A, *2*) the furanose ring conformation, *3*) the orientation of the ethynyl moiety, as described by the torsional angle ϕ_{CO} (C(6′/I)–C(5′/I)–C(4′/I)–O(4′/I)), and *4*) the nature of the propargylic substituent (OH or H) and the configuration at C(5′/I). We expected these parameters to remain decisive also for the formation of cyclic duplexes of the analogous ethenylene-linked dinucleosides, with steric interactions between the ribosyl moieties of units I and II conceivably also playing a role.

Maruzen models indicated that cyclic duplexes of (*Z*)-configured U*[c_e]A$^{(*)}$ and A*[c_e]U$^{(*)}$ dinucleosides can accommodate *Watson–Crick*, reverse *Watson–Crick*, *Hoogsteen*, or reverse *Hoogsteen* H-bonds. These models also suggest that cyclic duplexes show some conformational flexibility, characterized by a simultaneous change of the χ and ϕ_{CO} angles, and that the orientation of the ethenyl group in cyclic duplexes, as specified by the ϕ_{CO} angle, is limited to a *tg*- to *gt*-type conformation. In contradistinction to the U*[c_y]A$^{(*)}$ and A*[c_y]U$^{(*)}$ alkynes, the (*Z*)-configured U*[c_e]A$^{(*)}$ and A*[c_e]U$^{(*)}$ alkenes possessing a *gg*-oriented ethenyl moiety can only form linear duplexes and higher associates, but not cyclic duplexes. The (*E*)-configured U*[c_e]A$^{(*)}$ and A*[c_e]U$^{(*)}$ dinucleosides, however, must adopt a *gg*-orientation to form cyclic duplexes, characterized by an orthogonal orientation of the planes of the nucleobase and ethenyl moieties.

The association of the U*[c_e]A$^{(*)}$ and A*[c_e]U$^{(*)}$ dinucleosides in $CHCl_3$ solution was investigated by NMR and CD spectroscopy, similarly as described for the analysis of the U*[c_y]A$^{(*)}$ and A*[c_y]U$^{(*)}$ dinucleosides [2]. Association of the ethynylene-linked dinucleosides was revealed by the concentration dependence of the ^{1}H-NMR signals, and best quantified by analysing the concentration dependence of δ(HN(3)) of the uracil moiety. A large chemical shift difference ($\Delta\delta$) between the HN(3) signal of the simplex (extrapolation to $c = 0$ mM) and the duplex(es) ($c > 20$ mM), a strong bending of the curve at low concentration, and a curve progression resulting in a plateau at a higher concentration evidence the formation of cyclic duplexes, whereas a distinctly smaller $\Delta\delta$ value, a moderate bending of the curve at low concentration, and a continued dependence of the downfield shift on the concentration evidence linear duplexes and higher associates. Graphical analysis [3] or analysis by linear least-squares fitting [4] of these curves led in some cases to a strong deviation of the $\delta(NH_{simplex})$ value, especially in the U*[c_y]A$^{(*)}$ series, due to the absence of data for concentrations below 0.5 mM[3]). When this problem arose for the ethenylene-linked dimers, we introduced typical $\delta(NH_{simplex})$ values of 7.70 ppm in the U*[c_e]A$^{(*)}$ series and of 7.85 ppm in the A*[c_e]U$^{(*)}$ series for dilute (0.01 or 0.001 mM) solutions. This correction led to distinctly reduced confidence intervals for the *K* values.

The thermodynamic parameters of the association were obtained by *van't Hoff* plots, based on the temperature dependence of δ(HN(3)) for 3–5 mM solutions from 0

---

[3]) A satisfying signal/noise ratio was obtained by recording the ^{1}H-NMR spectra for 1 mM solutions overnight. At high dilution, the experimental δ(HN(3)) values are not accurate, as they are influenced by the H/H exchange with residual HDO in $CDCl_3$.

to 50° in 10° intervals. A thorough analysis of the ^{1}H- and ^{13}C-NMR spectra, recorded at a concentration where *ca.* 80% of the dinucleosides are in the form of duplexes, and of the concentration dependence of additional ^{1}H-NMR parameters (such as δ(H–C(2′/I)) and J(4′,5′/I)) allowed us to determine more precisely the conformation of duplexes. ROESY and circular dichroism (CD) spectra provided information about the type of base pairing and stacking, respectively. *Watson–Crick*-type base pairing was evidenced by a cross-peak between the signals of the uracil HN(3) and the adenine H–C(2). *Hoogsteen*-type base pairing was evidenced by the absence of this cross-peak, and by a cross-peak between the signals of the uracil HN(3) and the adenine H–C(8) of *C*(8/I)-unsubstituted U*[c$_e$]A dimers. Base stacking in cyclic duplexes was evidenced by a strong and constant decrease of the ellipticity of the CD signals upon increasing the temperature. The restrictions resulting from these analyses allowed us to generate appropriate *Maruzen* and AMBER* models of the cyclic duplexes.

We will first discuss observations valid for all U*[c$_e$]A$^{(*)}$ and A*[c$_e$]U$^{(*)}$ dimers, and then those that are specific for sets of U*[c$_e$]A$^{(*)}$ and A*[c$_e$]U$^{(*)}$ dinucleosides. In the U*[c$_e$]A$^{(*)}$ series, these are the (*Z*)- and (*E*)-*C*(5′/I)-deoxyalkenes, and the corresponding diastereoisomeric allyl alcohols, whereas all A*[c$_e$]U$^{(*)}$ dinucleosides will be discussed in parallel.

2.1. *NMR Parameters Relevant to Both U*[c$_e$]A$^{(*)}$ and A*[c$_e$]U$^{(*)}$ Dimers.* ^{1}H-NMR Spectra were recorded of 60 mM solutions in $CDCl_3$ of the dimers **8**, **10**, **14**, **16**, **17**, **19**, **21**, **23**, **25**, and **29**, of a 40 mM solution of **27**, and of a 25 mM solution of **6** (*Tables 8* and *10* in the *Exper. Part*). The dimer **12** shows severe line-broadening in $CDCl_3$; we thus analysed the NMR spectra of a 60 mM solution in $CDCl_3$/CD_3OD 10:1 where only the solvated simplex is expected [1]. The assignments are based on selective homodecoupling experiments, and corroborated by DQFCOSY and HSQC spectra of **14**, **17**, and **25**.

The (*Z*)-configuration of **6**, **8**, **10**, **12**, **14**, **16**, **19**, **21**, **23**, **25**, **27**, and **29** is evidenced by J(6′,7′/I) = 11.1–12.3 Hz, and the (*E*)-configuration of **17** by J(6′,7′/I) = 15.6 Hz. The different interactions of the nucleobases with the alkenyl moiety are evidenced by the upfield shift of the H–C(6′/I) and H–C(7′/I) signals of the U*[c$_e$]A$^{(*)}$ relative to those of the A*[c$_e$]U$^{(*)}$ dimers (*Tables 8* and *10* in the *Exper. Part*). C(6′/I) and C(7′/I) of the U*[c$_e$]A$^{(*)}$ dimers resonate at 135.3–138.3 and 122.0–124.5 ppm and those of the A*[c$_e$]U$^{(*)}$ dimers at 137.2–143.1 and 116.8–118.3 ppm, respectively (*Tables 9* and *11* in the *Exper. Part*).

The *syn*-conformation of unit II is evidenced by the downfield shift of H–C(2′/II), resonating at 5.19–5.43 ppm in the U*[c$_e$]A$^{(*)}$ series and at 5.62–5.75 ppm in the A*[c$_e$]U$^{(*)}$ series (*Tables 8* and *10* in the *Exper. Part*). The U* unit of the U*[c$_e$]A$^{(*)}$ dimers shows a stronger preference for the (*N*)-conformation than the A* unit of A*[c$_e$]U$^{(*)}$ dimers, as evidenced by J(1′,2′/II)/J(3′,4′/II) $\leq$ 0.30 and 0.64–0.75, respectively.

2.2. *Association of the U*[c$_e$]A$^{(*)}$ C(5′/I)-Deoxy (Z)-Alkenes* **14** *and* **16**: *Formation of* Watson–Crick *H-Bonded Cyclic Duplexes.* The strong concentration dependence of HN(3/II) ($\Delta\delta$ = 1.8–1.9 ppm; *Table 1*) and H_2N–C(6/I) ($\Delta\delta$ = 0.65–0.67 ppm) of the *C*(8)-unsubstituted **14** and the *C*(8)-silyloxymethylated **16** in $CDCl_3$ reveals a simplex/duplex equilibrium. The concentration dependence of HN(3/II) shows the typical curve progression of cyclic duplexes; *i.e.*, a large chemical-shift difference between

Table 1. *Concentration Dependence of the ^{1}H-NMR Chemical Shifts* [ppm] *of the U*[c$_e$]A$^{(*)}$ Dimers* **6**, **8**, **10**, **14**, **16**, *and* **17** *in CDCl$_3$* (highest concentration: δ value; lower concentrations: $\Delta\delta$ values relative to the highest concentration)[a])

	6			**8**			**10**		
Conc. [mM]	25	5	1	60	5	1	60	5	1
Uridine unit (II)									
HN(3)	12.19	−1.29	−2.71	12.78	−1.46	−2.28	12.50	−1.8	−3.16
H−C(5)	5.40	+0.03	+0.11	5.16	−0.08	+0.18	5.58	−0.01	+0.06
H−C(1′)	5.87	−0.02	−0.05	5.89	0	−0.01	5.83	−0.01	−0.02
H−C(2′)	5.28	−0.02	−0.04	5.29	+0.02	+0.01	5.43	−0.08	−0.16
Adenosine unit (I)									
H_2N−C(6)	6.71	−0.42	−0.75	6.78	−0.48	−0.70	7.04	−0.64	−1.05
H−C(2)	8.35	−0.01	−0.02	8.34	−0.02	−0.03	8.27	+0.03	+0.05
H−C(8)	7.97	−0.05	−0.08	–	–	–	7.90	0	0
H−C(1′)	5.96	−0.03	−0.06	6.52	−0.01	−0.02	6.01	−0.05	−0.09
H−C(2′)	5.20	−0.01	−0.03	5.22	−0.01	−0.02	5.43	−0.18	−0.25
H−C(3′)	5.28	−0.02	−0.09	5.39	−0.04	−0.09	5.13	−0.01	−0.02
HO−C(5′)	5.95	+0.11	+0.48	5.44	+0.22	+0.52	6.73	−0.04	+0.06[b])
	14			**16**			**17**		
Conc. [mM]	60	5	1	60	5	1	60	5	1
Uridine unit (II)									
HN(3)	13.37	−0.74	−1.81	13.38	−0.7	−1.87	12.03	−1.79	−3.07
H−C(5)	5.10	+0.02	+0.07	5.01	+0.04	+0.11	5.60	−0.01	+0.02
H−C(1′)	5.85	+0.01	−0.01	5.72	0	0	5.69	−0.02	−0.03
H−C(2′)	5.43	−0.03	−0.05	5.33	0	−0.03	5.32	−0.02	−0.07
Adenosine unit (I)									
H_2N−C(6)	7.04	−0.37	−0.67	6.95	−0.35	−0.65	6.59	−0.53	−0.83
H−C(2)	8.36	+0.01	0	8.30	−0.01	−0.01	8.39	0	−0.01
H−C(8)	7.90	−0.02	−0.02	–	–	–	7.96	−0.04	−0.07
H−C(1′)	6.02	0	0	6.62	−0.01	−0.03	6.04	0	−0.01
H−C(2′)	5.55	−0.01	−0.02	5.67	−0.02	−0.03	5.64	0	−0.04
H−C(3′)	5.13	0	−0.03	5.13	−0.01	−0.03	5.00	0	−0.01

[a]) $\Delta\delta > 0.03$ ppm between the highest and the lowest concentration are also observed for H−C(4′/I) of **6**, **14**, and **16** (+0.04, −0.05, and −0.07 ppm, resp.), and H−C(7′/I) of **8** and **10** (+0.06 and −0.06 ppm, resp.). [b]) Signal appears as *d* ($J = 9.3$ Hz).

simplex and duplex, a strong bending of the curve at concentrations between 1 and 10 mM, and a flattening of the curve (formation of a plateau) at concentrations above 30 mM (*Fig. 1,a*). A plateau at a chemical shift above 13 ppm is characteristic for *Watson–Crick*-type H-bonded cyclic duplexes [2].

Graphical analysis [3] of the curves in *Fig. 1,a* led to association constants (*K* values) of 3245 and 2250 M^{-1} for **14** and **16**, respectively (*Table 2*). *Van't Hoff* analysis of the temperature dependence gave ΔH values of −13.9 (for **14**) and −12.2 kcal/mol (for **16**). This corresponds to an energy gain of 3–3.5 kcal/mol per intermolecular H-bond and agrees well with the results in the U*[c$_y$]A$^{(*)}$ series [2].

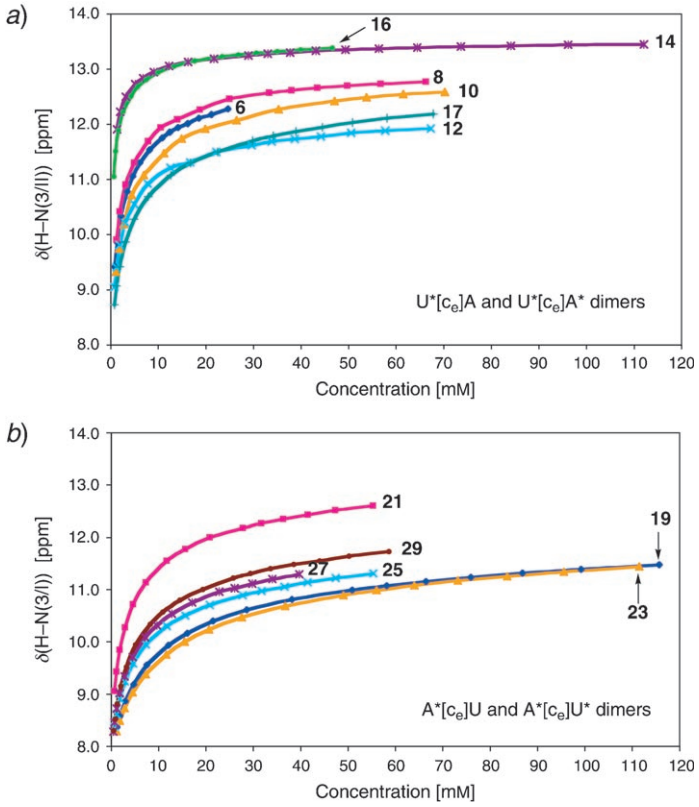

Fig. 1. *Concentration dependence of* a) δ*(HN(3/II)) of the U*[c_e]A(*) dimers* **6**, **8**, **10**, **12**, **14**, **16**, *and* **17**, *and* b) δ*(HN(3/I)) of the A*[c_e]U(*) dimers* **19**, **21**, **23**, **25**, **27**, *and* **29** *for solutions in* $CDCl_3$

The chemical shift for H–C(2′/I) of **14** and **16** (60 mM in $CDCl_3$), resonating at 5.55 and 5.67 ppm, respectively, evidences a predominantly and a completely *syn*-oriented adenine moiety (*Table 1*). The *syn*/*anti*-equilibria were not affected by dilution from 60 to 1 mM, as revealed by a very weak upfield shift of the H–C(2′/I) signals ($\Delta\delta \leq$ 0.03 ppm). The J(4′,5′a/I) and J(4′,5′b/I) values of **14** depend weakly upon the concentration (9.3 and 4.5 Hz for a 60 mM solution, 9.0 and 3.0 Hz for both a 5 and a 1 mM solution; *Table 3*). This evidences a *tg*- or *gt*-orientation of the ethenyl moiety in the cyclic duplex, as suggested by *Maruzen* models. The coupling constants J(4′,5′a/I) and J(4′,5′b/I) of **16** (8.4 and 5.1 Hz for a 60 mM solution, 7.5 and 6.6 Hz for a 1 mM solution) are rationalized by a *tg*/*gt*-equilibrium tending to a 1:1 ratio at high dilution.

Formation of a cyclic duplex of **14** is corroborated by vapor-pressure osmometric molecular weight determination for a 35 mM solution in $CHCl_3$. The resulting apparent molecular mass of 1431 ± 100 corresponds to an association degree of 1.89. Formation of a cyclic duplex is also supported by the evidence for π-stacking derived from the CD spectra of **14** (2 mM in $CHCl_3$) where one observes a strong decrease of the ellipticity upon increasing the temperature from -10 to 50° (*Fig. 2*). There is no exciton splitting.

Table 2. *Association Constant* K *and* δ(*NH*) *of the Simplex and the Duplex as Calculated from the Concentration Dependence of* δ(*HN(3)*) *in* $CDCl_3$ *at 295 K for the U*[c$_e$]A$^{(*)}$ Dimers* **6**, **8**, **10**, **12**, **14**, **16**, **17**, *and the A*[c$_e$]U$^{(*)}$ Dimers* **19**, **21**, **23**, **25**, **27**, *and* **29**[a]). Thermodynamic Parameters resulting from *van't Hoff* Analysis of the Temperature Dependence of δ(HN(3)) for 3–5 mM Solutions in $CDCl_3$ at 0–50° (in 10° steps).

Dimer	K [M^{-1}]	δ($NH_{simplex}$) [ppm]	δ(NH_{duplex}) [ppm]	ΔG_{298} [b]) [kcal/mol]	ΔH [kcal/mol]	ΔS [cal/mol·K]
U*[c$_e$]A$^{(*)}$ series						
6	375	7.66	13.47	−3.5	−8.7	−18.3
8	441	7.64	13.55	−3.6	−9.2	−19.1
10	255	7.67	13.47	−3.3	−7.4	−14.0
12	365	7.67	12.57	−3.5	−8.2	−15.9
14	3245	7.66	13.62	−4.8	−13.9	−31.3
16	2250	7.65	13.79	−4.6	−12.2	−26.3
17	173	7.71	13.17	−3.0	−9.3	−21.9
A*[c$_e$]U$^{(*)}$ series						
19	59	7.85	12.57	−2.4	−8.5	−21.0
21	220	7.86	13.62	−3.2	−11.0	−26.8
23	45	7.87	12.73	−2.3	−6.8	−15.8
25	107	7.85	12.44	−2.8	−7.6	−16.5
27	118	7.87	12.60	−2.8	−10.1	−24.8
29	117	7.83	12.91	−2.8	−10.2	−24.6

[a]) This calculation led to δ($NH_{simplex}$) values of 6.50–7.92 ppm in the U*[c$_e$]A$^{(*)}$ series and of 7.82–8.10 ppm in the A*[c$_e$]U$^{(*)}$ series. An additional shift value of 7.70 and 7.85 ppm for 0.01M solutions (**14** and **16**: 0.001M) of the U*[c$_e$]A$^{(*)}$ and A*[c$_e$]U$^{(*)}$ series, respectively, led to more reliable δ($NH_{simplex}$) values and to distinctly smaller confidence intervals (*K:* ≤7.7%; δ($NH_{simplex}$) and δ(NH_{duplex}): ≤ 0.07 ppm). [b]) Calculated from *K*.

The 262 nm UV band of **14** reflects the combined absorption by the adenine λ_{max} *ca.* 260 nm) and the ethenylated uridine moieties (expected λ_{max} *ca.* 270 nm)[4]).

A strong cross-peak between the signals of H–C(2/I) and HN(3/II) in the ROESY spectrum of 22 mM **14** in $CDCl_3$ corroborates the *Watson–Crick*-type base pairing of the cyclic duplex.

Plausible starting geometries for force-field calculations of the structure of the cyclic duplexes were estimated by *Maruzen* modeling. Modeling of the two *Watson–Crick* and the two reverse *Watson–Crick* base-paired cyclic duplexes of **14** and **16** suggested a *syn*-oriented adenine and a *tg*-oriented ethenyl moiety (see **UA1** to **UA4** in *Fig. 3*). **UA2** and **UA4** are destabilized by steric interactions between the uridine ribosyl units, or between the uridine ribosyl unit and the adenine moiety (marked with stars). Hence, force-field calculation was restricted to **UA1** and **UA3**.

---

4) There is only partial conjugation in this (*Z*)-configured alkene, as evidenced by the λ_{max} values of (*Z*)- and (*E*)-6-(2-bromoethenyl)-2,3-*O*-isopropylideneuridines (271 *vs.* 279 nm [5]) and the corresponding iodides (267 *vs.* 282 nm [5]); no UV data are available for the corresponding 6-(alk-1-enyl)uridines.

Table 3. *Concentration Dependence of* $^3J(4,5/I)$ *of the U*[c$_e$]A$^{(*)}$ Dimers* **6**, **8**, **10**, **14**, **16**, *and* **17**, *and of the A*[c$_e$]U$^{(*)}$ Dimers* **19**, **21**, **23**, **25**, **27**, *and* **29** *in* $CDCl_3$

U*[c$_e$]A$^{(*)}$ Dimer	Conc. [mM]	$J(4',5'_a/I)$ [Hz]	$J(4',5'_b/I)$ [Hz]	A*[c$_e$]U$^{(*)}$ Dimer	Conc. [mM]	$J(4',5'_a/I)$ [Hz]	$J(4',5'_b/I)$ [Hz]
6	1	3.3	–	**19**	1	4.2	–
	5	3.9	–		5	4.2	–
	25	4.5	–		60	3.9	–
8	1	3.6	–	**21**	1	6.9	–
	5	5.1	–		5	7.8	–
	60	5.7	–		60	8.7	–
10	1	1.8	–	**23**	1	3.3	–
	5	2.1	–		5	3.6	–
	60	3.6	–		60	3.9	–
14	1	9.0	3.0	**25**	1	6.6	–
	5	9.0	3.0		5	6.6	–
	60	9.3	4.5		60	6.9	–
16	1	7.5	6.6	**27**	1	6.6	6.6
	5	8.1	5.4		5	6.9	6.9
	50	8.4	5.1		40	6.9	6.9
17	1	6.3	6.3	**29**	1	6.6	6.6
	5	6.0	6.0		5	6.9	6.9
	60	6.1	6.1		60	6.9	6.9

AMBER* modeling [6] of the **UA1** duplex of **14** reduced the distance between the base pairs to *ca.* 3.2 Å (relative to the one for the *Maruzen* model) by changing the χ and ϕ_{CO} angles (*Fig. 4* and *Table 4*). After optimization, the adenine moiety adopted a *syn*-orientation ($\chi = +51.5°$) and the ethenyl moiety a *gt*-orientation ($\phi_{CO} = +60$ and $+96°$). The two different ϕ_{CO} values suggest some flexibility of the duplex. Modeling of the **UA1** duplex of **16** led to a similar structure, evidencing a negligible influence of the substituent at C(8/I). AMBER* modeling of the **UA3** duplex of **14**, possessing reverse *Watson–Crick* H-bonds, resulted in an *anti*-orientation of the adenine unit ($\chi = -129°$) and a *gt*-orientation ($\phi_{CO} = +88.5°$) of the ethenyl moiety. The small upfield shift for H–C(2′/I) of **14** ($\Delta\delta = 0.12$ ppm relative to H–C(2′/I) of **16**, see above) suggests that the cyclic duplexes of **14** are predominantly connected by *Watson–Crick* and, to a smaller extent, by reverse *Watson–Crick* H-bonding. The U*[c$_e$]A* dimer **16** can only form a *Watson–Crick* H-bonded duplex, as the *syn*-conformation is imposed by the substituent at C(8/I).

ROESY Cross-peaks between the signals of H–C(3′/I) and H–C(3′/II) of **14**, and between the signals of H–C(2/I) and those of H–C(2′/II), H–C(3′/II), and of the more deshielded H–C(5′/I) corroborate the *Watson–Crick* H-bonding (ROEs indicated in *Fig. 4* by double-headed arrows). ROESY Cross-peaks between the signals of H–C(8/I) and those of both H–C(2′/II) and the more deshielded H–C(5′/I) of **14** are due to a reverse *Watson–Crick* H-bonded duplex, whereas cross-peaks between the signals of C(5′/II)H_2 and those of both H–C(2/I) and H–C(8/I) could neither be assigned to a linear nor to a cyclic duplex.

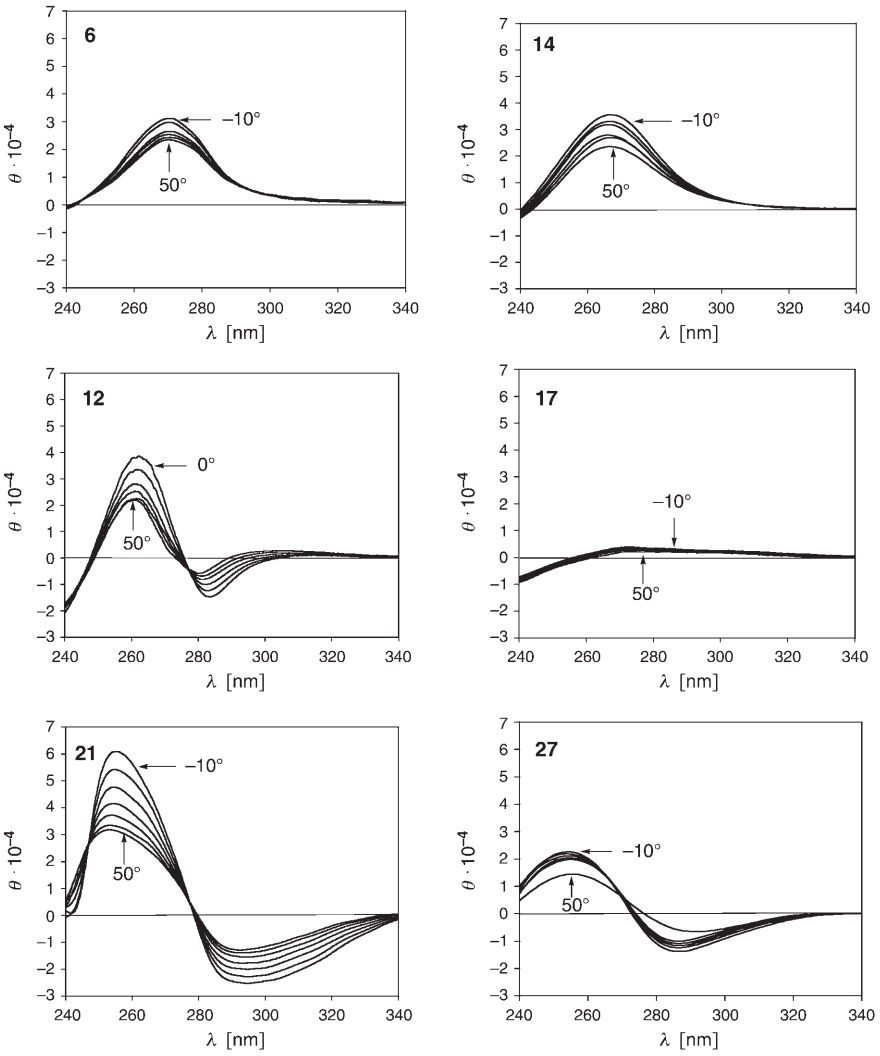

Fig. 2. *CD Spectra recorded in 10° steps from −10 to 50° for 2 mM solutions of* **6**, **12**, **14**, **17**, *and* **27**, *and 1 mM solution of* **21** *in* $CHCl_3$

2.3. *Association of the U*[c_e]A* C*(5′/I)-Deoxy (*E*)-Alkene* **17**: *Formation of Linear Duplexes.* The curve describing the concentration dependence of HN(3/II) of **17** shows the progression typical for linear duplexes and higher associates, *viz.* a moderate chemical-shift difference between simplex and duplex, a weak bending of the curve at concentrations of 1 to 10 mM, and a continued constant increase of the downfield shift at concentrations above 30 mM (*Fig. 1,a*).

Graphical analysis of the curve in *Fig. 1,a* led to a K value of $173\,M^{-1}$ for **17** (*Table 2*). This value and the thermodynamic parameters cannot be accurate, as the

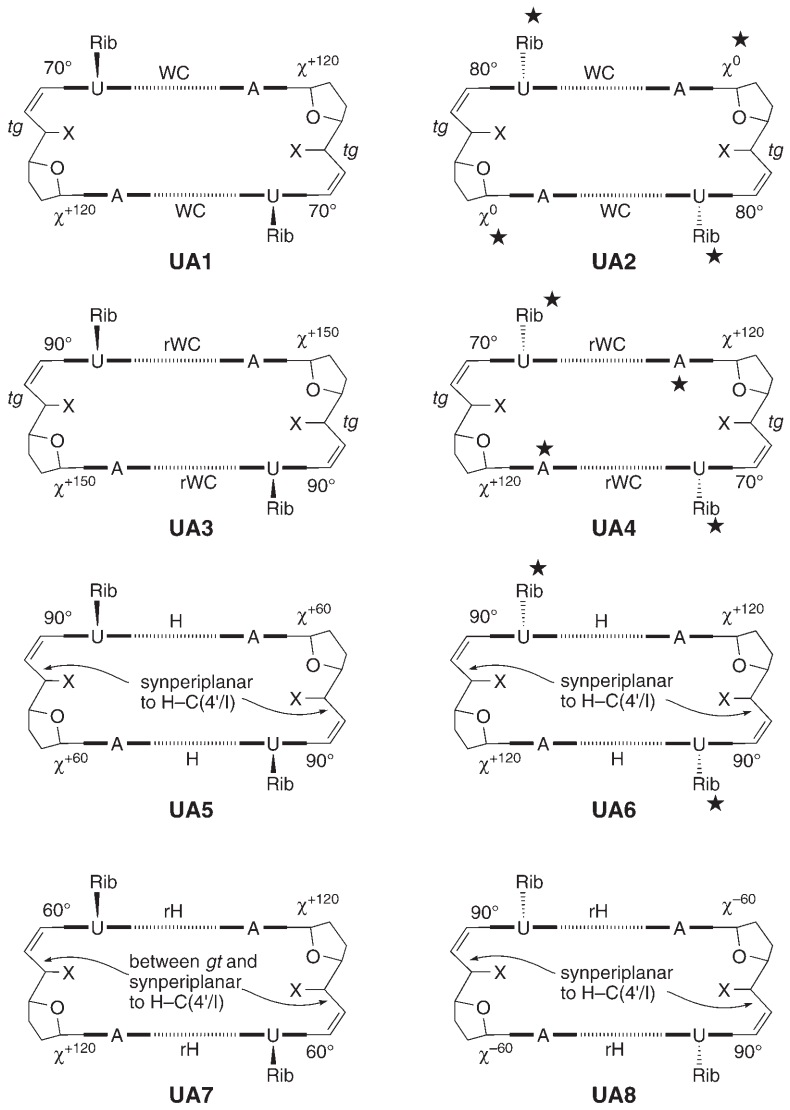

Fig. 3. Maruzen-*modeled* C_2*-symmetric cyclic duplexes of U*[*c_e*]A(*) dimers connected by* Watson–Crick (*WC*), *reverse* Watson–Crick (r*WC*), Hoogsteen (*H*), *and reverse* Hoogsteen (r*H*) *base pairing: schematic representations showing the orientation of the adenine and ethenyl moieties* (relative to both the furanose ring of unit I and the uridine moiety), *and destabilizing steric interactions* (marked with a star)

graphical determination is based on a constant $\delta(NH_{duplex})$ value. A ΔH value of *ca.* −7 kcal/mol is expected for linear duplexes. The rather large ΔH value of **17** (−9.3 kcal/mol) suggests the formation of minor amounts of higher associates.

The *syn*-orientation of the adenine unit of **17** in 1–60 mM solutions in $CDCl_3$ is evidenced by the downfield shift of H–C(2′/I), resonating at 5.60–5.64 ppm (*Table 1*).

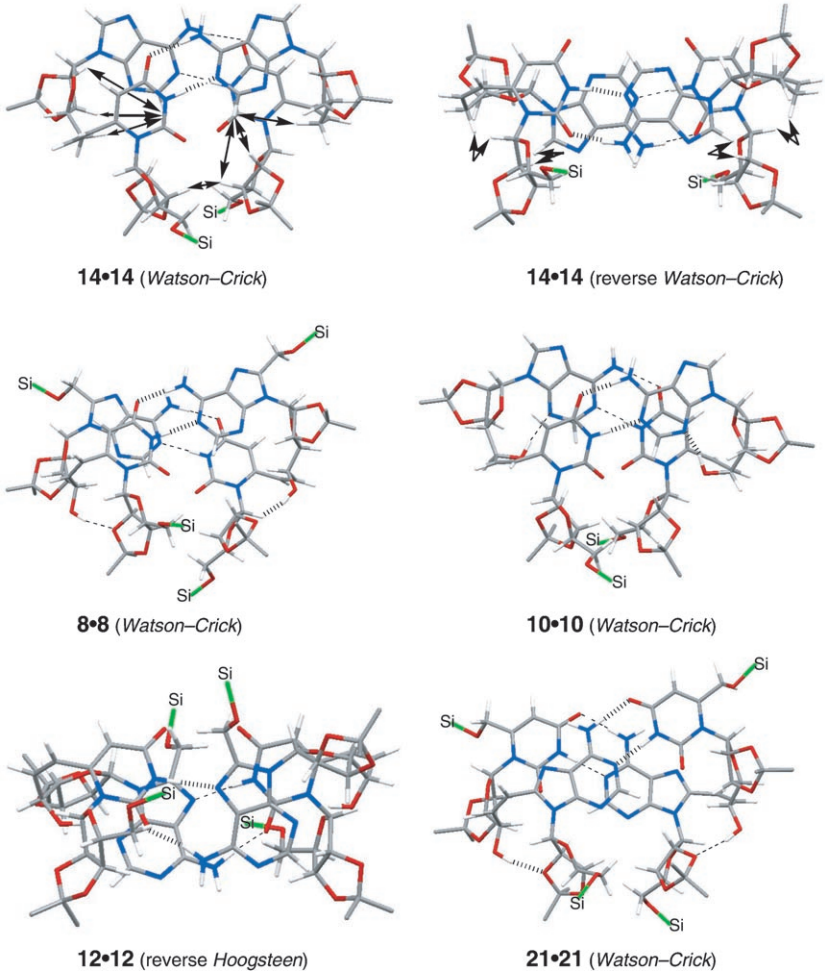

Fig. 4. AMBER*-*modeled U*[c_e]$A^{(*)}$ cyclic duplexes connected by* Watson–Crick (**8**·**8**, **10**·**10**, **14**·**14**, and **21**·**21**), *reverse* Watson–Crick (**14**·**14**), *and reverse* Hoogsteen (**12**·**12**) *base pairing: H-bonds marked with hashed* (base pair in the foreground) *and dashed* (base pair in the background) *bonds* (the substituents at Si- and the isopropylidene H-atoms are omitted to enhance visibility). ROEs are indicated by double-headed arrows.

The *J*(4′,5′a/I) and *J*(4′,5′b/I) values of **17** are independent of the concentration. Their values (6.1–6.3 Hz; *Table 3*) evidence a 1:1:1 *gg*/*gt*/*tg*-equilibrium and a free rotation about the C(4′/I)–C(5′/I) bond, implying the absence of cyclic duplexes.

The CD spectrum of **17** (2 mM solution in $CHCl_3$; *Fig. 2*) shows a very weak ellipticity, corroborating the formation of only linear duplexes. In agreement with a similar observation for U*[c_y]$A^{(*)}$ dimers [2], the linear duplexes of **17** possess *Watson–Crick*- and *Hoogsteen*-type H-bonds, as evidenced by ROESY cross-peaks

Table 4. *Selected Distances* [Å] *and Torsion Angles* [°] *of U*[c_e]A$^{(*)}$ Duplexes Connected by* Watson–Crick (**14**·**14**, **8**·**8**, **10**·**10**), *reverse* Watson–Crick (**14**·**14**), *and reverse* Hoogsteen (**12**·**12**) *H-Bonds*

Duplex	**14**·**14** (*WC*)	**14**·**14** (r*WC*)	**8**·**8** (*WC*)	**10**·**10** (*WC*)	**12**·**12** (r*H*)
Distance N(3/II)H···N(1 or 7/I)	1.75	1.78	1.76	1.77	1.82
Distance NH···O=C(4 or 2/II)	1.74, 1.78	1.71	1.745	1.72	1.685
Distance O(5′/I)H···N(3/I)	–	–	–	1.82	1.845
Distance O(5′/I)H···O(2′/II)	–	–	1.83	–	–
Distance between base pairs	3.2	3.3	3.2	3.25	3.5
χ of unit I	+51.5	−129	+52	+49	+58.5
ϕ_{CO} of unit I (∠ C(6′/I)–C(5′/I)–C(4′/I)–O)	+96, +60	+88.5	+59.5	+61	+67.5
ϕ_{OO} of unit I (∠ O–C(5′/I)–C(4′/I)–O)	–	–	+177	−64.5	−57.5
∠ N(1/II)–C(6/II)–C(7′/I)–C(6′/I)	−78	−73	−78	−86	−76
χ of unit II	+61.5	+67	+58	+65	+71.5
Propeller twist	1	5	1	4	32, 33

between the signals of HN(3/II), and those of H–C(2/I) and H–C(8/I). The intensity of the cross-peaks suggests a *ca.* 3 : 1 ratio of the *Watson–Crick*- and *Hoogsteen*-type H-bonded duplexes.

2.4. *Association of the U*[c_e]A$^{(*)}$ Allyl Alcohols* **6**, **8**, **10**, *and* **12**: *Formation of Linear and Cyclic Duplexes.* The curves describing the concentration dependence of HN(3/II) of **6**, **8**, **10**, and **12** resemble the one of **17**, exhibiting a moderate chemical-shift difference between simplex and duplex, and a weak bending of the curve at concentrations of 1 to 10 mM (*Fig. 1*,*a*). However, a distinct flattening of the curves of **8**, **10**, and **12** is observed at concentrations above 30 mM. An insufficient solubility of **6** did not allow a determination of δ(HN(3/II)) at concentrations above 25 mM. Thus, the curve progression of **8**, **10**, and **12** evidences an equilibrium between the simplex, and linear and cyclic duplexes. This is probably also the case for **6**, as suggested by the similarity of the curves of **6**, **8**, and **10** at concentrations below 25 mM. The distinctly smaller downfield shift for HN(3/II) of **12** as compared to the one for HN(3/II) of **6**, **8**, and **10** suggests *Hoogsteen*-type H-bonds in the cyclic duplex of **12** and *Watson–Crick*-type H-bonds in the cyclic duplexes of **6**, **8**, and **10**.

Graphical analysis of the curves of **6**, **8**, **10**, and **12** in *Fig. 1*,*a* led to *K* values of 255–441 M^{-1} (*Table 2*). $\delta(NH_{duplex})$ Values of 13.47–13.55 ppm evidence *Watson–Crick*-type base pairing of the cyclic duplexes of **6**, **8**, and **10**, whereas a $\delta(NH_{duplex})$ value 12.57 ppm reveals *Hoogsteen*-type base pairing of the cyclic duplexes of **12**. The presence of minor amounts of cyclic duplexes and higher associates for **6**, **8**, **10**, and **12** is suggested by ΔH values of −7.4 to −9.2 kcal/mol.

HO–C(5′/I) of **6**, **8**, and **10** resonates as a broad *s*, preventing the determination of *J*(5′,OH/I) (*Table 8* in the *Exper. Part*). The line broadening suggests an equilibrium of H-bonded species. Upon dilution to 1 mM, the HO–C(5′/I) signal of **6** and **8** is shifted downfield by *ca.* 0.5 ppm, whereas the signal of **10** does not move much (*Table 1*). This evidences that the intramolecular H-bond to N(3/I) persists in the cyclic duplex of **10**, but is replaced by another intra- or intermolecular H-bond in the cyclic duplexes of **6**

and **8**[5]). A change of H-bonding is also suggested by the observation that the $J(4',5'/I)$ value of **6** and **8** increases more strongly with increasing concentration than the $J(4',5'/I)$ value of **10** (**6**: 3.3 to 4.5, **8**: 3.6 to 5.7, **10**: 1.8 to 3.6 Hz; *Table 3*).

The decrease of ellipticity upon increasing the temperature from -10 to 50° that characterizes the CD spectrum of **6** (2 mM in $CHCl_3$) evidences π-stacking, as typically found in cyclic duplexes (*Fig. 2*). The similar shape of the CD spectra of **6** and **14** suggests *Watson–Crick*-type base pairing in the cyclic duplexes also of **6**. Severe line-broadening for HN(3/II) of **6** prevented the detection of NOESY cross-peaks with H–C(2/I) and H–C(8/I), and the confirmation of the type of H-bonding. The presence of cyclic duplexes of **12** is corroborated by a decrease of ellipticity upon increasing temperature. The shape of the CD spectrum of **12** differs from the one of **6** and **14** by a negative absorption at 285 nm, suggesting a different base pairing, presumably of a *Hoogsteen*-type, as concluded above from the weaker downfield shift of HN(3/II).

A cyclic duplex of **10** resembling the *Watson–Crick* base-paired duplex of **14** should also have a *gt*-oriented ethenyl and, hence, a *gg*-oriented OH group, as required to form an intramolecular H-bond to N(3/I). This H-bond is indeed maintained in the AMBER* modeling of the *Watson–Crick* H-bonded cyclic duplex of **10** (*Fig. 4* and *Table 4*). One expects that the cyclic duplex of **12** also prefers a *Watson–Crick* type H-bonding, although there is precedent for a switching from *Watson–Crick* to *Hoogsteen* base pairing upon introduction of a $CH_2OSi^tBuPh_2$ substituent, albeit in a uridine moiety [2]. *Maruzen* modeling suggested that the *Hoogsteen*-type H-bonded duplex **UA7** is favoured over the duplexes **UA5** (destabilizing steric interaction of the $CH_2OSi^tBuPh_2$ substituent), **UA6** (destabilizing steric interaction between the uridine ribosyl units), and **UA8** (*anti*-oriented 8-substituted adenine moiety; *Fig. 3*). AMBER* modeling of the **UA8** duplex of **12** maintains the intramolecular H-bond of HO–C(5′/I) to N(3/I) (*Fig. 4* and *Table 5*). A propeller twist of 32–33° results from the intermolecular steric interaction between the CH_2 group of the $CH_2OSi^tBuPh_2$ substituent and O=C(4/II). This interaction could be stabilized by an intermolecular C(8/I)CH···O=C(4/II) H-bond, as suggested by calculations with the semiempiric programme AM1 [8], resulting in a propeller twist of 7°. A larger $\Delta\delta$ value for CH_2–C(8/I) of **12** than that of **16** is suggested by this C–H···O H-bond, and observed for a 20 mM solution of **12** in $CDCl_3$ at $-10°$[6]).

A *Watson–Crick* base-paired cyclic duplex of the D-*allo*-configured dimers **6** and **8** that is similar to the one of **14** should have a *gt*-oriented ethenyl and a *tg*-oriented OH group that is incompatible with an intramolecular H-bond to N(3/I). This conformation

---

5) The lower persistence of the intramolecular H-bond to N(3/I) in the U*[c_e]A(*) than in the U*[c_y]A(*) series reflects the lower acidity of allyl alcohols (*cf.* pK_{HA} of 15.5 and 13.55 for allyl and propargyl alcohol, respectively [7]).

6) Two sharp *d*s ($J = 13.2$ Hz) at 4.98 and 4.94 ppm are observed for CH_2–C(8/I) of a 20 mM solution of **12** at 50°. They disappear at room temperature due to coalescence. At $-10°$, a *d* corresponding to one of the H-atoms of the CH_2–C(8/I) group appears at 4.64 ppm ($J = 13.5$ Hz). The weak asymmetry of this *d* evidences that the *d* of the coupling partner is far away, presumably hidden by other signals at 5.35 ppm. The large $\Delta\delta \approx 0.6$ ppm at $-10°$ suggests that one CH–C(8/I) acts as H-donor in the cyclic duplex, whereas the small $\Delta\delta = 0.04$ ppm (compare with 0.11 ppm for **16** at room temperature) at 50° evidences the presence of only linear duplexes at this temperature.

Table 5. *Concentration Dependence of the ^{1}H-NMR Chemical Shifts* [ppm] *of the A*[c_e]U$^{(*)}$ Dimers* **19**, **21**, **23**, **25**, **27**, *and* **29** *in $CDCl_3$* (highest concentration: δ value; lower concentrations: $\Delta\delta$ values relative to the highest concentration)[a])

	19			**21**			**23**		
Conc. [mM]	60	5	1	60	5	1	60	5	1
Adenosine unit (II)									
$H_2N-C(6)$	6.34	−0.56	−0.79	6.68	−0.67	−0.89	6.31	−0.54	−0.72
H−C(2)	8.37	−0.01	−0.02	8.30	+0.03	+0.03	8.36	−0.02	−0.03
H−C(1′)	6.20	+0.01	+0.02	6.19	−0.01	−0.01	6.14	0	0
H−C(2′)	5.62	0	0	5.63	0	+0.01	5.74	+0.05	+0.07
Uridine unit (I)									
HN(3)	11.07	−1.88	−2.7	12.60	−2.32	−3.18	11.08	−2.05	−2.79
H−C(5)	5.76	−0.03	−0.02	5.56	+0.05	+0.06	5.68	0	0
H−C(1′)	5.85	+0.01	+0.03	5.98	−0.08	−0.11	5.85	+0.03	+0.06
H−C(2′)	4.95	−0.06	−0.07	5.29	−0.05	−0.09	4.94	−0.01	−0.04
H−C(3′)	5.08	−0.02	−0.04	5.38	−0.10	−0.11	5.07	−0.03	−0.05
H−C(5′)	4.94	−0.04	−0.06	4.85	0	+0.01	5.08	−0.14	−0.18
HO−C(5′)	6.40	+0.10	+0.10	6.29	−0.03	−0.03	5.89	+0.09	+0.18[b])
	25			**27**			**29**		
Conc. [mM]	60	5	1	40	5	1	60	5	1
Adenosine unit (II)									
$H_2N-C(6)$	6.43	−0.38	−0.62	6.36	−0.38	−0.59	6.48	−0.40	−0.64
H−C(2)	8.28	0	+0.01	8.25	+0.01	+0.03	8.14	+0.05	+0.10
H−C(1′)	6.17	−0.01	−0.01	6.14	0	+0.01	6.12	+0.01	+0.01
H−C(2′)	5.68	+0.02	+0.04	5.71	0	0	5.75	+0.01	+0.02
Uridine unit (I)									
HN(3)	11.37	−1.66	−2.71	11.30	−1.6	−2.58	11.73	−1.79	−2.92
H−C(5)	5.61	+0.01	+0.02	5.70	−0.02	−0.02	5.61	+0.01	+0.02
H−C(1′)	5.90	−0.01	−0.02	5.50	+0.03	+0.06	5.87	−0.03	−0.04
H−C(2′)	5.25	−0.05	−0.06	5.08	−0.02	−0.05	5.26	−0.02	−0.03
H−C(3′)	5.25	−0.05	−0.06	4.93	−0.01	−0.02	5.06	0	0
H−C(5′)	5.38	−0.10	−0.16	3.43	−0.01	−0.01	3.47	+0.01	+0.02
HO−C(5′)	4.91	+0.15	+0.25	–	–	–	–	–	–

[a]) $\Delta\delta > 0.03$ ppm between the highest and the lowest concentration are also observed for $H_a-C(5'/II)$ of **21** (+0.06 ppm), and H−C(6′/I) of **23** and **25** (+0.07 and +0.06 ppm, resp.). [b]) Signal appears as *d* (J = 3.3 Hz).

(antiperiplanar H−C(4′/I) and H−C(5′/I)) agrees with the observed concentration-dependent increase of J(4′,5′/I) (see above). AMBER* modeling of the *Watson–Crick* H-bonded duplex of **8**, corresponding to **UA1** in *Fig. 3*, led to such a structure and to the formation of an intramolecular H-bond of HO−C(5′/I) to O−C(2′/II) (*Fig. 4* and *Table 4*).

2.5. *Association of the A*[c_e]U$^{(*)}$ Dimers* **19**, **21**, **23**, **25**, **27**, *and* **29**: *Formation Mostly of Linear Duplexes.* The curve for the concentration dependence of HN(3/I) of **19**, **21**, **23**, **25**, **27**, and **29** shows the progression typical of linear duplexes and higher associates discussed above (*Fig. 1*, *b*). The *C*(6/I)-unsubstituted allyl alcohols **19** and **23** form only

linear duplexes and higher associates, with the uridine unit adopting an *anti*-orientation (see below). The alcohols indeed show the weakest downfield shift for HN(3/I). Substantial amounts of cyclic, *Watson–Crick*-type H-bonded duplexes of **21** are evidenced by the relatively strong downfield shift for HN(3/I) ($\geq$12.5 ppm for concentrations above 60 mM). The curves describing the concentration dependence of the chemical shift for HN(3/I) of **25**, **27**, and **29** show an intermediate downfield shift relative to the curves of **21**, **19**, and **23**. This is rationalized by the presence of either small amounts of *Watson–Crick*-type H-bonded duplexes, or substantial amounts of *Hoogsteen*-type H-bonded duplexes, although the downfield shift for **25** and **29** may also be affected by the substitution at C(6/I). The presence of small amounts of *Watson–Crick*-type H-bonded duplexes appears more probable, since the curves do not show the characteristic flattening (as observed for **12**). The similar CD spectra of **21** and **27** indeed evidence *Watson–Crick*-type H-bonding for both duplexes (*Fig. 2*). The presence of only small amounts of cyclic duplexes of **27** is evidenced by the weak ellipticity of a 2 mM solution of **27**, as compared to a 1 mM solution of **21**. There is no exciton splitting. The A*[c_e]U$^{(*)}$ and A*[c_y]U$^{(*)}$ dimers show UV maxima at 263–270 (U unit) and 292–306 nm (8-substituted A unit), corresponding to the CD maxima and evidencing an unimpaired conjugation between the adenine and (*Z*)-ethenyl moieties.

Graphical analysis of the curves in *Fig. 1*,*b* led to *K* values of 45–59 M^{-1} for **19** and **23**, 107–118 M^{-1} for **25**, **27**, and **29**, and 220 M^{-1} for **21** (*Table 2*). These values and the thermodynamic parameters are not accurate, as the graphical analysis is based on a constant $\delta(NH_{duplex})$ value. The formation of substantial amounts of *Watson–Crick*-type base-paired cyclic duplexes by **21** is evidenced by $\delta(NH_{duplex}) = 13.62$ ppm. Association of the L-*talo*-configured dimers **23** and **25** is characterized by the smallest ΔH values (−6.8 to −7.6 kcal/mol), typical for linear duplexes. The larger values for **19** (−8.5 kcal/mol), and for **21**, **27**, and **29** (−10.1 to −11.0 kcal/mol) evidence substantial amounts of higher associates and/or cyclic duplexes.

For 60 mM solutions in $CDCl_3$, H−C(2′/I) of the C(6/I) unsubstituted allyl alcohols **19** and **23** resonates at 4.94–4.95 ppm, revealing the *anti*-orientation of the uracil moiety (*Table 5*). The downfield shift for H−C(2′/I) (5.08 ppm) of the corresponding deoxy analogue **27** suggests a *ca.* 1:1 *syn*/*anti*-equilibrium. As expected, the *C*(6/I)-substituted A*[c_e]U* dimers **21**, **25**, and **29** (H−C(2′/I) at 5.25–5.29 ppm) adopt completely a *syn*-conformation. Hence, only **21**, **25**, **27**, and **29** can form cyclic duplexes. Upon dilution to 1 mM, the signal for H−C(2′/I) of all A*[c_e]U$^{(*)}$ dimers is only slightly shifted upfield ($\Delta\delta = 0.03–0.09$ ppm).

J(4′,5′a/I) and *J*(4′,5′b/I) of **27** and **29** are identical and independent of the concentration (*Table 3*). Their value (6.6–6.9 Hz) evidences a 1:1 *gt*/*tg*-orientation of the ethenyl moiety. As expected, steric interactions with the uracil moiety prevent the population of the *gg*-conformation. This facilitates the conformational analysis of the allyl alcohols **19**, **21**, **23**, and **25**, as only two staggered conformations must be considered. The *J*(4′,5′a/I) value of **21** decreases from 8.7 Hz for a 60 mM solution to 6.9 Hz for a 1 mM solution. This evidences a *gt*-orientation of the ethenyl moiety in the cyclic duplex and a 1:1 *gt*/*tg*-conformational equilibrium in the simplex. The *J*(4′,5′a/I) values of **19**, **23**, and **25** depend only weakly upon the concentration ($\Delta J \leq 0.6$ Hz), and agree well with the dominant (**25**) or exclusive (**19** and **23**) presence of linear duplexes

and higher associates. The $J(4',5'a/I)$ values of the A*[c_y]U dimers **19** and **23** are small (≤ 4.2 Hz), evidencing that the OH group and not the H-atom is preferentially *gg*-oriented in these uridines adopting the *anti*-conformation, as suggested by the steric interaction with the uracil moiety. The *gg*-orientation of the OH group may be rationalized by the *gauche*-effect and by an intramolecular H-bond to O–C(4′). However, the downfield shift of HO–C(5′/I) (**19**: 6.40, **23**: 5.89 ppm; *Table 5*) suggests that also N(7/II) acts as H-bond acceptor either in a bifurcated or a flip-flop H-bond. The chemical shifts for HO–C(5′/I) of the A*[c_y]U* dimers **21** (6.29 ppm) and **25** (4.91 ppm) confirm the stronger H-bonding to N(7/II) in the D-*allo*-series.

The ROESY spectra of the A*[c_e]U dimers **19** and **27** corroborate the *Watson–Crick*-type H-bonding by cross-peaks between the signals of HN(3/I) and H–C(2/II). In view of the missing H–C(8/II), they cannot evidence *Hoogsteen*-type H-bonding that is also expected in linear duplexes.

Maruzen modeling of the A*[c_e]U$^{(*)}$ duplexes can be restricted to *Watson–Crick*-type H-bonding. The duplex **AU1** is favoured over **AU2** to **AU4**, as these duplexes are destabilized by an eclipsed orientation of the ethenyl moiety (*Fig. 5*).

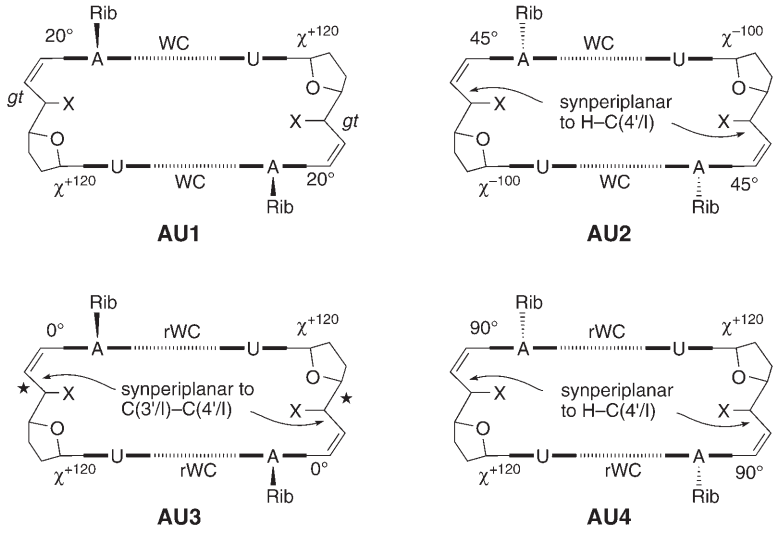

Fig. 5. Maruzen-*modeled* C_2-*symmetric cyclic duplexes of A*[c_e]U$^{(*)}$ dimers connected by* Watson–Crick (*WC*), and *reverse* Watson–Crick (r*WC*) *base pairing: schematic representations showing the orientation of the adenine and ethenyl moieties* (relative to both the furanose ring of unit I and the uridine moiety), *and destabilizing steric interactions* (marked with a star)

AMBER* modeling of the **AU1** duplex of **21** resulted in a cyclic duplex possessing a *syn*-oriented uracil ($\chi = +58°$), a *tg*-oriented ethenyl ($\phi_{CO} = +50°$), a *gt*-oriented OH group ($\phi_{OO} = +169°$), and an antiperiplanar H–C(4′/I) and H–C(5′/I) (*Fig. 4* and *Table 6*). This conformation agrees well with the large $J(4',5'/I)$ value (8.7 Hz for a 60 mM solution). HO–C(5′/I) is engaged in an intramolecular H-bond to O–C(2′/II).

The C(5′/I)-deoxy analogues **27** and **29** which cannot form such a H-bond show a lower tendency to form *Watson–Crick* H-bonded duplexes. In spite of the inversion of the configuration at C(5′/I) of **25** it is still possible to form a H-bond from HO–C(5′/I) to O–C(2′/II) in the corresponding *Watson–Crick* H-bonded cyclic duplex. However, the structure of this duplex was not analyzed in more detail, as **25** shows only a weak tendency to form cyclic duplexes.

Table 6. *Selected Distances* [Å] *and Torsion Angles* [°] *of the A*[c$_e$]U* Duplex* **21**·**21** *Connected by* Watson–Crick *H-Bonds*

Duplex	**21**·**21** (*WC*)
Distance N(3/I)H···N(1/II)	1.765
Distance NH···O=C(4/I)	1.75
Distance O(5′/I)H···O(2′/II)	1.835, 1845
Distance between base pairs	3.2
χ of unit I	+58
ϕ_{CO} of unit I (∠ C(6′/I)–C(5′/I)–C(4′/I)–O)	+50
ϕ_{OO} of unit I (∠ O–C(5′/I)–C(4′/I)–O)	+169
∠ N(9/II)–C(8/II)–C(7′/I)–C(6′/I)	−61
χ of unit II	+59
Propeller twist	2
Buckle twist	16, 17.5

2.6. *Comparison of the Helical Structures of the* Watson–Crick *Base-Paired Cyclic Duplexes of the C(5/I)-Deoxygenated Dimers.* There is a striking difference between the stability of the cyclic duplexes of the U*[c$_e$]A$^{(*)}$ and A*[c$_e$]U$^{(*)}$ series, best evidenced by the association constants of the *Watson–Crick* base-paired cyclic duplexes of the *C*(5′/I)-deoxy dimers. The cyclic U*[c$_e$]A$^{(*)}$ duplexes **14**·**14** and **16**·**16** (K = 3254 and 2250 M^{-1}, resp.) are far more stable than the A*[c$_e$]U$^{(*)}$ duplexes **27**·**27** and **29**·**29** (K = 117–118 M^{-1}; *Table 7*). A similar difference is observed for the sequence isomeric alkynes, but here it depends upon the substitution of unit I. This is seen by comparing, on the one hand, the stability of the U*[c$_y$]A and A*[c$_y$]U duplexes **13**·**13** and **26**·**26** (K = 1159 and 277 M^{-1}, resp. [2]) and, on the other hand, of the U*[c$_y$]A* and A*[c$_y$]U* duplexes **15**·**15** and **28**·**28** (K = 973 and 1793 M^{-1}, resp. [2]). Modeling showed that substitution of unit I has no influence upon the helical structure

Table 7. *Comparison of the Helical Structure of the* Watson–Crick *Base-Paired Cyclic Duplexes* **13**·**13** *to* **16**·**16** *and* **26**·**26** *to* **29**·**29**

Duplex (K [M^{-1}])	**13**·**13** (1159) **15**·**15** (973)	**14**·**14** (3245) **16**·**16** (2250)	**26**·**26** (277) **28**·**28** (1793)	**27**·**27** (118) **29**·**29** (117)
Type	U*[c$_y$]A$^{(*)}$	U*[c$_e$]A$^{(*)}$	A*[c$_y$]U$^{(*)}$	A*[c$_e$]U$^{(*)}$
Sense of rotation	left	left	left	left
Orientation of nucleobase of unit I	*syn*	*syn*	*syn*	*syn*
Orientation of ethynyl or ethenyl moiety	*gg*	*gt*	*gg*	*gt*
Axial rise [Å]	3.4	3.2	3.45	3.2
Twist [°]	13	36	67	60
Residues per turn	27.7	10	5.4	6

of the duplexes. All these *Watson–Crick* base-pairing cyclic duplexes form left-handed helices, possess a *syn*-oriented nucleobase, and show a similar distance between the base pairs (3.2–3.45 Å). The ethenyl moiety adopts a *gt*- and the ethynyl moiety a *gg*-orientation.

The main difference between the UA and AU series is the attachment of the linker to the five-membered imidazole ring in the UA dimers and to the six-membered pyrimidine ring in the AU dimers. This leads to different twist angles, small (13°) for the U*[c_y]A(*) duplexes, moderate (36°) for the U*[c_e]A(*), and large for the A*[c_e]U(*) (60°) and A*[c_y]U(*) (67°) duplexes, resulting in a different number of residues per helical turn (27.7, 10, 6, and 5.4, resp.). It also leads to a different extent of π-stacking of the base pairs; *i.e.*, a good stacking of U with the pyrimidine part of A in the U*[c_y]A(*) and A*[c_y]U(*) duplexes, a moderate stacking in the U*[c_e]A(*) duplexes, and a poor one in A*[c_e]U(*) duplexes with only the N(1/II)–C(2/II) bonds superimposed.

The analysis shows that the base sequence, *i.e.*, the orientation of the linker resulting from its attachment to a specific nucleobase, the orientation of the nucleobase, the structure of the linker, and its orientation relative to the furanosyl ring have a strong influence upon the helical structure of the cyclic duplexes. The propensity of a specific dimer to form cyclic duplexes is thus not easy to predict, and this all the more so, as all *Watson–Crick*- and *Hoogsteen*-type base pairings have to be taken into consideration.

We thank the *ETH Zürich* and *F. Hoffmann-La Roche AG*, Basel, for generous support, Mrs. *B. Brandenberg* for recording the 2D-NMR spectra, and Prof. *B. Jaun* for helpful discussions.

Experimental Part

General. See [9]. For NMR titrations and *van't Hoff* analysis, see [2].

2′,3′-O-*Isopropylidene-5′*-O-*(triisopropylsilyl)uridin-6-yl-(6 → 7′*-C*)-(6′*Z*)-9-(6,7-dideoxy-2,3*-O-*isopropylidene-β*-D-allo-*hept*-6-*enofuranosyl)adenine* (**6**). A suspension of **5** [2] (200 mg, 0.26 mmol) and 10% Pd/C (150 mg) in MeOH (60 ml) was stirred under H_2 (5 bar) for 12 h at 25°. Filtration through *Celite*, evaporation, and FC ($CHCl_3$/MeOH 16:1) gave **6** (114 mg, 57%). White solid. R_f ($CHCl_3$/MeOH 16:1) 0.25. M.p. 160–162°. $[\alpha]_D^{25} = +10.8$ ($c = 0.5$, $CHCl_3$). UV ($CHCl_3$): 262.0 (14200). IR ($CHCl_3$): 3411*w* (br.), 3180*w* (br.), 3015*s*, 1696*s*, 1634*s*, 1383*m*, 1251*w*, 1088*s*, 931*w*, 880*w*. ^{1}H-NMR (500 MHz, $CDCl_3$): see *Table 8*; additionally, 1.64, 1.55, 1.39, 1.36 (4*s*, 2 Me_2C); 1.05–0.99 (*m*, $(Me_2CH)_3Si$). ^{13}C-NMR (125 MHz, $CDCl_3$): see *Table 9*; additionally, 114.29, 113.93 (2*s*, 2 Me_2C); 27.45, 27.31, 25.54, 25.38 (4*q*, 2 Me_2C); 18.00, 17.99 (2*q*, $(Me_2CH)_3Si$); 12.02 (*d*, $(Me_2CH)_3Si$). HR-MALDI-MS: 794.3530 ($[M+Na]^+$, $C_{36}H_{53}N_7NaO_{10}Si^+$; calc. 794.3521).

2′,3′-O-*Isopropylidene-5′*-O-*(triisopropylsilyl)uridin-6-yl-(6 → 7′*-C*)-(6′*Z*)-8-{[(*tert*-butyl)diphenylsilyloxy]methyl}-9-(6,7-dideoxy-2,3*-O-*isopropylidene-β*-D-allo-*hept*-6-*enofuranosyl)adenine* (**8**). A suspension of **7** [2] (30 mg, 0.029 mmol), 5% Pd/$BaSO_4$ (30 mg), and quinoline (30 mg, 0.23 mmol) in MeOH (9 ml) was stirred under H_2 (1 bar) for 1 h at 25°. Filtration through *Celite*, evaporation, and FC ($CHCl_3$/MeOH 40:1) gave **8** (28 mg, 92%). White solid. R_f ($CHCl_3$/MeOH 20:1) 0.31. M.p. 151–153°. $[\alpha]_D^{25} = +36.9$ ($c = 2.0$, $CHCl_3$). UV ($CHCl_3$): 265.0 (23600). IR ($CHCl_3$): 3410*w* (br.), 3200*w* (br.), 3017*s*, 2866*m*, 1693*m*, 1638*m*, 1449*w*, 1376*m*, 1263*w*, 1220*s*, 1157*w*, 1084*s*, 880*w*, 823*w*. ^{1}H-NMR (300 MHz, $CDCl_3$): see *Table 8*; additionally, 7.70–7.64 (*m*, 4 arom. H); 7.46–7.33 (*m*, 6 arom. H); 1.61, 1.55, 1.38, 1.37 (4*s*, 2 Me_2C); 1.07 (*s*, Me_3C); 1.04–0.98 (*m*, $(Me_2CH)_3Si$). ^{13}C-NMR (75 MHz, $CDCl_3$): see *Table 9*; additionally, 135.54 (*d*, 4 C); 132.26, 132.14 (2*s*); 129.89, 129.84 (2*d*); 127.75 (*d*, 2 C); 127.67 (*d*, 2 C); 114.20, 113.98 (2*s*, 2 Me_2C); 27.43, 27.23, 25.55, 25.38 (4*q*, 2 Me_2C); 26.77 (*q*, Me_3C); 19.31 (*s*, Me_3C); 17.99, 17.97 (2*q*, $(Me_2CH)_3Si$); 12.00 (*d*, $(Me_2CH)_3Si$). HR-MALDI-MS: 1062.478 ($[M+Na]^+$, $C_{53}H_{73}N_7NaO_{11}Si_2^+$; calc. 1062.480).

Table 8. *Selected ^{1}H-NMR Chemical Shifts* [ppm] *and Coupling Constants* [Hz] *for 60 mM Solutions of the U*[c$_e$]A$^{(*)}$ Dimers* **6**, **8**, **10**, **12**, **14**, **16**, *and* **17** *in* $CDCl_3$[a])

	6[b])	**8**	**10**	**12**[c])	**14**[d])	**16**	**17**[d])
Uridine unit (II):							
HN(3)	12.19	12.78	12.50	–	13.37	13.38	12.03
H–C(5)	5.40	5.16	5.58	5.68	5.10	5.01	5.60
H–C(1′)	5.87	5.89	5.83	5.71	5.85	5.72	5.69
H–C(2′)	5.26	5.29	5.43	5.19	5.43	5.33	5.32
H–C(3′)	4.88	4.89	4.89	4.79	4.89	4.89	4.88
H–C(4′)	4.13	4.15	4.18	4.07	4.03	4.11	4.18
H_a–C(5′)	3.91	3.90	3.87	3.81	3.90	3.86	3.89
H_b–C(5′)	3.87	3.86	3.83	3.77	3.85	3.81	3.86
^4J(5,NH)	< 2.0	< 2.0	< 2.0	–	0	0	0
J(1′,2′)	1.2	1.2	< 1.5	1.2	< 1.5	1.2	1.1
J(2′,3′)	6.3	6.6	6.3	6.3	6.3	6.3	6.3
J(3′,4′)	4.2	3.9	4.2	5.1	5.1	4.2	4.2
J(4′,5′$_a$)	5.4	5.7	5.7	5.4	4.8	5.4	5.6
J(4′,5′$_b$)	6.3	7.2	6.3	6.6	6.0	6.9	7.0
J(5′$_a$,5′$_b$)	10.8	10.5	10.8	10.8	10.8	10.5	10.5
Adenosine unit (I):							
NH_2–C(6)	6.71	6.5–7.0	7.04	–	6.6–7.5	6.7–7.2	6.59
H–C(2)	8.35	8.34	8.27	8.15	8.36	8.30	8.39
H–C(8)	7.97	–	7.90	–	7.90	–	7.96
CH_a–C(8)	–	4.99	–	4.91	–	5.01	–
CH_b–C(8)	–	4.93	–	4.81	–	4.92	–
H–C(1′)	5.96	6.52	6.01	6.39	6.02	6.62	6.04
H–C(2′)	5.20	5.22	5.43	5.14	5.55	5.67	5.64
H–C(3′)	5.30	5.39	5.13	5.04	5.13	5.13	5.00
H–C(4′)	4.33	4.22	4.47	4.33	4.41	4.37	4.34
H_a–C(5′)	4.74	4.71	4.55	4.52	2.94	2.77	2.70
H_b–C(5′)	–	–	–	–	2.49	2.50	2.65
HO–C(5′)	5.8–6.1	5.44	6.73	–	–	–	–
H–C(6′)	6.07	6.06	6.09	6.10	5.95	5.97	6.21
H–C(7′)	6.38	6.28	6.38	6.26	6.31	6.19	6.31
J(H_a,H_b)	–	13.2	–	13.2	–	12.9	–
J(1′,2′)	3.0	2.4	1.2	4.5	0	< 1.0	2.0
J(2′,3′)	6.3	6.3	6.3	6.3	6.3	6.3	6.4
J(3′,4′)	2.1	3.3	1.8	2.1	2.7	3.3	4.3
J(4′,5′$_a$)	4.5	5.7	3.6	2.1	9.3	8.4	6.1
J(4′,5′$_b$)	–	–	–	–	4.5	5.1	6.1
J(5′$_a$,5′$_b$)	–	–	–	–	14.7	15.3	15.2
J(5′$_a$,OH)	[e])	[e])	[e])	–	–	–	–
J(5′$_a$,6′)	8.7	9.0	7.8	9.6	9.6	8.1	6.5
J(5′$_b$,6′)	–	–	–	–	5.7	6.6	6.5
J(6′,7′)	11.7	11.4	11.7	11.4	11.1	11.1	15.6

[a]) Assignments based on selective homodecoupling experiments. [b]) 25 mM Solution. [c]) In $CDCl_3$/CD_3OD 10 : 1 (severe line broadening in $CDCl_3$). [d]) Assignments based on a DQFCOSY and a HSQC spectrum. [e]) Not determined.

Table 9. *Selected* ^{13}*C-NMR Chemical Shifts* [ppm] *of the U*[c$_c$]A$^{(*)}$ Dimers* **6**, **8**, **10**, **12**, **14**, **16**, *and* **17** *in* $CDCl_3$

	6	**8**	**10**	**12**[a])	**14**[b])	**16**	**17**[b])
Uridine unit (II):							
C(2)	150.63	150.43	151.56	151.02	151.04	150.60	151.08
C(4)	162.92	163.22	163.68	163.02	163.30	163.47	163.80
C(5)	102.85	102.55	103.06	103.14	103.51	103.06	101.59
C(6)	148.13	149.49	147.95	149.24	148.37	149.87	153.54
C(1′)	92.45	92.74	93.07	92.38	91.23	92.39	92.47
C(2′)	83.82	83.89	83.86	83.88	83.61	83.87	83.96
C(3′)	81.78	82.25	82.04	81.81	81.03	82.16	82.30
C(4′)	88.67	88.76	89.34	89.15	87.94	87.72	89.43
C(5′)	63.90	63.98	64.32	64.06	63.45	64.08	64.30
Adenosine unit (I):							
C(2)	152.43	151.80	152.09	152.05	152.37	151.68	153.18
C(4)	150.40	150.20	150.44	150.28	150.11	150.53	149.22
C(5)	120.30	118.70	120.22	118.24	119.95	118.58	119.91
C(6)	155.94	155.88	156.24	155.60	156.16	155.79	155.96
C(8)	140.03	149.06	140.06	149.04	140.39	149.50	140.30
CH_2–C(8)	–	59.70	–	59.64	–	60.00	–
C(1′)	92.14	90.44	92.73	91.82	90.76	89.71	90.31
C(2′)	84.16	84.57	83.28	82.94	84.50	84.58	83.82
C(3′)	80.99	81.54	82.04	81.63	84.50	84.50	83.10
C(4′)	89.20	89.12	89.34	87.00	88.21	89.02	85.42
C(5′)	68.54	69.53	69.53	68.97	34.05	34.08	36.02
C(6′)	137.63	138.30	137.41	135.35	135.56	135.84	136.49
C(7′)	123.60	123.10	122.79	122.07	123.48	122.76	124.51

[a]) In $CDCl_3/CD_3OD$ 10:1. [b]) Assignments based on HSQC spectrum.

2′,3′-O-*Isopropylidene-5′*-O-*(triisopropylsilyl)uridin-6-yl-(6 → 7′*-C*)-(6′*Z*)-9-(6,7-dideoxy-2,3*-O-*isopropylidene-α*-L-talo-*hept*-6-*enofuranosyl)adenine* (**10**). A suspension of **9** [2] (106 mg, 0.138 mmol), 5% $Pd/BaSO_4$ (53 mg), and quinoline (26 mg, 0.2 mmol) in MeOH (28 ml) was stirred under H_2 (1 bar) for 3 h at 25°. Filtration through *Celite*, evaporation, and FC ($CHCl_3$/MeOH 30:1) gave **10** (100 mg, 94%). White solid. R_f ($CHCl_3$/MeOH 20:1) 0.20. M.p. 170–172°. $[\alpha]_D^{25} = -14.7$ ($c = 2.0$, $CHCl_3$). UV ($CHCl_3$): 265 (26100). IR ($CHCl_3$): 3411*w* (br.), 3184*w* (br.), 3017*s*, 2944*m*, 2867*m*, 1701*s*, 1635*s*, 1605*m*, 1431*m*, 1384*m*, 1335*w*, 1241*m*, 1156*m*, 1082*s*, 996*w*, 880*m*. ^{1}H-NMR (300 MHz, $CDCl_3$): see *Table 8*; additionally, 1.57, 1.45, 1.30, 1.28 (4*s*, 2 Me_2C); 0.98–0.91 (*m*, $(Me_2CH)_3Si$). ^{13}C-NMR (75 MHz, $CDCl_3$): see *Table 9*; additionally, 114.22, 113.42 (2*s*, 2 Me_2C); 27.45, 27.33, 25.81, 25.21 (4*q*, 2 Me_2C); 17.96 (*q*, $(Me_2CH)_3Si$); 12.01 (*d*, $(Me_2CH)_3Si$). HR-MALDI-MS: 794.3537 ($[M+Na]^+$, $C_{36}H_{53}N_7NaO_{10}Si^+$; calc. 794.3521). Anal. calc. for $C_{36}H_{53}N_7O_{10}Si$ (771.93): C 56.01, H 6.92, N 12.70; found: C 55.74, H 6.86, N 12.44.

2′,3′-O-*Isopropylidene-5′*-O-*(triisopropylsilyl)uridin-6-yl-(6 → 7′*-C*)-(6′*Z*)-8-{[(*tert-*butyl)diphenylsilyloxy]methyl}-9-(6,7-dideoxy-2,3*-O-*isopropylidene-α*-L-*talo-*hept*-6-*enofuranosyl)adenine* (**12**). A suspension of **11** [2] (30 mg, 0.029 mmol), 5% $Pd/BaSO_4$ (30 mg), and quinoline (30 mg, 0.23 mmol) in MeOH (9 ml) was stirred under H_2 (1 bar) for 3 h at 25°. Filtration through *Celite*, evaporation, and FC ($CHCl_3$/MeOH 40:1) gave **12** (23 mg, 76%). White solid. R_f ($CHCl_3$/MeOH 30:1) 0.14. M.p. 148–150°. $[\alpha]_D^{25} = -9.0$ ($c = 1.0$, $CHCl_3$). UV ($CHCl_3$): 266 (23000). IR ($CHCl_3$): 3486*w*, 3410*w* (br.), 3182*w* (br.), 2943*m*, 2866*m*, 1698*s*, 1639*s*, 1609*w*, 1454*w*, 1483*m*, 1333*w*, 1266*m*, 1156*m*, 1083*s*, 881*m*, 823*w*. ^{1}H-NMR (300 MHz, $CDCl_3/CD_3OD$ 10:1): see *Table 8*; additionally, 7.67–7.64 (*m*, 4 arom. H); 7.40–7.29 (*m*, 6

arom. H); 1.50, 1.45, 1.29, 1.28 (4*s*, 2 Me_2C); 1.01 (*s*, Me_3C); 0.98–0.92 (*m*, $(Me_2CH)_3Si$). ^{13}C-NMR (75 MHz, $CDCl_3$): see *Table 9*; additionally, 135.35 (*d*, 4 C); 131.97, 131.84 (2*s*); 129.85 (*d*, 2 C); 127.67 (*d*, 2 C); 127.63 (2*d*); 114.23, 113.42 (2*s*, 2 Me_2C); 27.48, 27.24, 25.42, 25.29 (4*q*, 2 Me_2C); 26.70 (*q*, Me_3C); 19.21 (*s*, Me_3C); 17.82 (*q*, $(Me_2CH)_3Si$); 12.00 (*d*, $(Me_2CH)_3Si$). HR-MALDI-MS: 1062.482 ($[M+Na]^+$, $C_{53}H_{73}N_7NaO_{11}Si_2^+$; calc. 1062.480).

2′,3′-O-*Isopropylidene-5′*-O-*(triisopropylsilyl)uridin-6-yl-(6 → 7′*-C*)-(6′*Z*)-9-(5,6,7-trideoxy-2,3*-O-*isopropylidene-β*-D-ribo-*hept*-6-*enofuranosyl)adenine* (**14**). A suspension of **13** [2] (30 mg, 0.04 mmol), 5% $Pd/BaSO_4$ (30 mg), and quinoline (30 mg, 0.23 mmol) in MeOH (9 ml) was stirred under H_2 (1 bar) for 1 h at 25°. Filtration through *Celite*, evaporation, and FC ($CHCl_3$/MeOH 30:1) gave **14** (28 mg, 92%). White solid. R_f ($CHCl_3$/MeOH 20:1) 0.20. M.p. 139–141°. $[\alpha]_D^{25} = +70.0$ ($c = 1.0$, $CHCl_3$). UV ($CHCl_3$): 262 (19100). IR ($CHCl_3$): 3486*w*, 3321*w*, 3184*w*, 2993*m*, 2944*m*, 2867*m*, 1706*s*, 1639*s*, 1603*m*, 1438*m*, 1384*m*, 1157*m*, 1092*s*, 874*m*. ^{1}H-NMR (500 MHz, $CDCl_3$): see *Table 8*; additionally, 1.61, 1.55, 1.42, 1.39 (4*s*, 2 Me_2C); 1.03–0.97 (*m*, $(Me_2CH)_3Si$). ^{13}C-NMR (125 MHz, $CDCl_3$): see *Table 9*; additionally, 113.76 (*s*, 2 Me_2C); 27.50, 27.06, 25.82, 25.30 (4*q*, 2 Me_2C); 17.99, 17.98 (2*q*, $(Me_2CH)_3Si$); 12.03 (*d*, $(Me_2CH)_3Si$). HR-MALDI-MS: 778.3534 ($[M+Na]^+$, $C_{36}H_{53}N_7NaO_9Si^+$; calc. 778.3572). Anal. calc. for $C_{36}H_{53}N_7O_9Si$ (755.93): C 57.20, H 7.07, N 12.97; found: C 56.91, H 7.02, N 12.83.

2′,3′-O-*Isopropylidene-5′*-O-*(triisopropylsilyl)uridin-6-yl-(6 → 7′*-C*)-(6′*Z*)-8-{[(*tert-*butyl)diphenylsilyloxy]methyl}-9-(5,6,7-trideoxy-2,3*-O-*isopropylidene-β*-D-ribo-*hept*-6-*enofuranosyl)adenine* (**16**). A suspension of **15** [2] (63 mg, 0.062 mmol), 5% $Pd/BaSO_4$ (60 mg), and quinoline (60 mg, 0.46 mmol) in MeOH (12 ml) was stirred under H_2 (1 bar) for 40 min at 25°. Filtration through *Celite*, evaporation, and FC ($CHCl_3$/MeOH 40:1) gave **16** (23 mg, 76%). White solid. R_f ($CHCl_3$/MeOH 20:1) 0.37. M.p. 129–131°. $[\alpha]_D^{25} = +38.5$ ($c = 2.0$, $CHCl_3$). UV ($CHCl_3$): 265 (14300). IR ($CHCl_3$): 3411*w* (br.), 3200*w*, 3017*s*, 2943*m*, 2866*m*, 1713*s*, 1637*m*, 1445*m*, 1383*m*, 1158*w*, 1083*s*, 879*m*, 824*w*. ^{1}H-NMR (300 MHz, $CDCl_3$): see *Table 8*; additionally, 7.74–7.63 (*m*, 4 arom. H); 7.48–7.31 (*m*, 6 arom. H); 1.62, 1.52, 1.40, 1.38 (4*s*, 2 Me_2C); 1.06 (*s*, Me_3C); 1.01–0.96 (*m*, $(Me_2CH)_3Si$). ^{13}C-NMR (75 MHz, $CDCl_3$): see *Table 9*; additionally, 135.60 (*d*, 2 C); 135.55 (*d*, 2 C); 132.30, 132.25 (2*s*); 129.89, 129.79 (2*d*); 127.76 (*d*, 2 C); 127.64 (*d*, 2 C); 113.57, 113.33 (2*s*, 2 Me_2C); 27.49, 27.22, 25.87, 25.46 (4*q*, 2 Me_2C); 26.84 (*q*, Me_3C); 19.33 (*s*, Me_3C); 18.00 (*q*, $(Me_2CH)_3Si$); 12.04 (*d*, $(Me_2CH)_3Si$). HR-MALDI-MS: 1046.478 ($[M+Na]^+$, $C_{53}H_{73}N_7NaO_{10}Si_2^+$; calc. 1046.486).

2′,3′-O-*Isopropylidene-5′*-O-*(triisopropylsilyl)uridin-6-yl-(6 → 7′*-C*)-(6′*E*)-9-(5,6,7-trideoxy-2,3*-O-*isopropylidene-β*-D-ribo-*hept*-6-*enofuranosyl)adenine* (**17**). A soln. of **14** (57 mg, 0.075 mmol) and I_2 (5 mg, 0.02 mmol) in toluene (3.5 ml) was irradiated by Hg light (250–300 nm) for 24 h. The soln. was diluted with CH_2Cl_2 (15 ml), washed with 10% aq. $Na_2S_2O_3$ soln. and brine (2 × 10 ml), dried (Na_2SO_4), and evaporated. FC ($CHCl_3$/MeOH 300:1) gave **17** (50 mg, 88%). White solid. R_f (nitrile TLC: $CHCl_3$/MeOH 200:1) 0.29. M.p. 138–140°. $[\alpha]_D^{25} = -8.0$ ($c = 1.0$, $CHCl_3$). UV ($CHCl_3$): 264 (15800). IR ($CHCl_3$): 3487*w*, 3411*w* (br.), 3200*w* (br.), 2944*m*, 2867*m*, 1690*s*, 1633*s*, 1603*m*, 1472*m*, 1384*m*, 1330*m*, 1157*m*, 1089*s*, 995*w*, 881*m*. ^{1}H-NMR (500 MHz, $CDCl_3$): see *Table 8*; additionally, 1.62, 1.52, 1.40, 1.34 (4*s*, 2 Me_2C); 1.05–1.00 (*m*, $(Me_2CH)_3Si$). ^{13}C-NMR (125 MHz, $CDCl_3$): see *Table 9*; additionally, 114.81, 113.45 (2*s*, 2 Me_2C); 27.26, 25.46 (2*q*, 2 Me_2C); 17.90 (*q*, $(Me_2CH)_3Si$); 11.98 (*d*, $(Me_2CH)_3Si$). HR-MALDI-MS: 778.3530 ($[M+Na]^+$, $C_{36}H_{53}N_7NaO_9Si^+$; calc. 778.3572).

2′,3′-O-*Isopropylidene-5′*-O-*(triisopropylsilyl)adenosin-8-yl-(8 → 7′*-C*)-(6′*Z*)-1-(6,7-dideoxy-2,3*-O-*isopropylidene-β*-D-allo-*hept*-6-*enofuranosyl)uracil* (**19**). A suspension of **18** [2] (106 mg, 0.138 mmol), 5% $Pd/BaSO_4$ (50 mg), and quinoline (50 mg, 0.39 mmol) in MeOH (30 ml) was stirred under H_2 (1 bar) for 30 min at 25°. Filtration through *Celite*, evaporation, and FC ($CHCl_3$/MeOH 40:1) gave **19** (50 mg, 47%). White solid. R_f ($CHCl_3$/MeOH 30:1) 0.12. M.p. 150–152°. $[\alpha]_D^{25} = +49.4$ ($c = 1.0$, $CHCl_3$). UV ($CHCl_3$): 263 (13000), 301 (9770). IR ($CHCl_3$): 3412*w* (br.), 3185*w* (br.), 3026*w*, 2944*m*, 2868*m*, 1696*s*, 1634*s*, 1456*m*, 1384*m*, 1334*w*, 1270*m*, 1157*m*, 1088*s*, 882*w*, 808*w*. ^{1}H-NMR (300 MHz, $CDCl_3$): see *Table 10*; additionally, 1.60, 1.59, 1.39, 1.37 (4*s*, 2 Me_2C); 1.02–0.94 (*m*, $(Me_2CH)_3Si$). ^{13}C-NMR (75 MHz, $CDCl_3$): see *Table 11*; additionally, 114.48, 114.28 (2*s*, 2 Me_2C); 27.21, 27.17, 25.40, 25.27 (4*q*, 2 Me_2C); 17.83 (*q*, $(Me_2CH)_3Si$); 11.81 (*d*, $(Me_2CH)_3Si$). HR-MALDI-MS: 794.3542 ($[M+Na]^+$, $C_{36}H_{53}N_7NaO_{10}Si^+$; calc. 794.3521).

2′,3′-O-*Isopropylidene-5′*-O-*(triisopropylsilyl)adenosin-8-yl-(8 → 7′*-C*)-(6′*Z*)-6-{[(*tert-*butyl)diphenylsilyloxy]methyl}-1-(6,7-dideoxy-2,3*-O-*isopropylidene-β*-D-allo-*hept*-6-*enofuranosyl)uracil* (**21**). A

Table 10. *Selected ^{1}H-NMR Chemical Shifts* [ppm] *and Coupling Constants* [Hz] *for 60 mM Solutions of the A*[c$_c$]U$^{(*)}$ Dimers* **19**, **21**, **23**, **25**, **27**, *and* **29** *in* $CDCl_3$ [a])

	19	**21**	**23**	**25**[b])	**27**[c])	**29**
Adenosine unit (II):						
NH_2–C(6)	6.30–6.40	6.5–6.9	6.31	6.43	6.36	6.48
H–C(2)	8.37	8.30	8.36	8.28	8.25	8.14
H–C(1′)	6.20	6.19	6.14	6.17	6.14	6.12
H–C(2′)	5.62	5.63	5.74	5.68	5.71	5.75
H–C(3′)	5.13	5.11	5.16	5.15	5.15	5.16
H–C(4′)	4.25	4.22	4.28	4.25	4.24	4.25
H_a–C(5′)	3.86	3.82	3.82	3.83	3.83	3.80
H_b–C(5′)	3.74	3.66	3.71	3.73	3.70	3.67
J(1′,2′)	2.4	2.4	2.4	2.7	2.1	2.1
J(2′,3′)	6.6	6.3	6.6	6.3	6.3	6.3
J(3′,4′)	3.6	3.6	3.3	3.6	3.3	3.3
J(4′,5′$_a$)	5.7	5.7	6.0	6.0	6.0	6.3
J(4′,5′$_b$)	5.4	5.7	6.0	5.7	5.7	6.0
J(5′$_a$,5′$_b$)	10.8	10.5	10.2	10.5	10.8	10.5
Uridine unit (I):						
HN(3)	11.07	12.60	11.08	11.37	11.30	11.73
H–C(5)	5.76	5.56	5.68	5.61	5.70	5.61
H–C(6)	7.63	–	7.68	–	7.21	–
CH_a–C(6)	–	4.59	–	4.59	–	4.60
CH_b–C(6)	–	4.38	–	4.38	–	4.40
H–C(1′)	5.85	5.98	5.85	5.90	5.50	5.87
H–C(2′)	4.95	5.29	4.94	5.21–5.27	5.08	5.26
H–C(3′)	5.08	5.38	5.07	5.21–5.27	4.93	5.06
H–C(4′)	4.38	4.29	4.45	4.38	4.31	4.25
H_a–C(5′)	4.94	4.85	5.08	5.38	3.43	3.47
H_b–C(5′)	–	–	–	–	3.04	2.95
HO–C(5′)	6.2–6.6	6.2–6.4	5.89	4.85–5.00	–	–
H–C(6′)	6.35	6.44	6.45	6.32	6.22	6.21
H–C(7′)	6.81	6.70	6.78	6.75	6.66	6.59
J(5,6)	8.1	–	8.1	–	8.4	–
J(H_a,H_b)	–	13.5	–	13.8	–	13.8
J(1′,2′)	2.4	< 1.5	2.7	< 1.0	1.8	< 1.0
J(2′,3′)	6.6	6.3	6.3	[d])	6.6	6.3
J(3′,4′)	3.3	3.9	3.6	2.4	4.5	4.8
J(4′,5′$_a$)	3.9	8.7	3.9	6.9	6.9	6.9
J(4′,5′$_b$)	–	–	–	–	6.9	6.9
J(5′$_a$,5′$_b$)	–	–	–	–	14.7	15.0
J(5′$_a$,OH)	< 2.0	[d])	[d])	[d])	–	–
J(5′$_a$,6′)	6.3	6.0	6.9	7.5	7.5	7.5
J(5′$_b$,6′)	–	–	–	–	7.5	7.5
J(5′$_a$,7′)	1.5	< 1.5	1.2	< 1.0	0	0
J(6′,7′)	12.3	12.0	12.0	11.7	11.7	11.7

[a]) Assignments based on selective homodecoupling experiments. [b]) Assignments based on a DQFCOSY and a HSQC spectrum. [c]) 40 mM Solution. [d]) Not determined.

Table 11. *Selected ^{13}C-NMR Chemical Shifts* [ppm] *of the A*[c$_c$]U$^{(*)}$ Dimers* **19**, **21**, **23**, **25**, **27**, *and* **29** *in $CDCl_3$*

	19	**21**	**23**	**25**[a])	**27**	**29**
Adenosine unit (II):						
C(2)	153.16	152.36	152.88	152.64	152.41	151.95
C(4)	149.79	149.48	149.46	149.49	150.24	149.21
C(5)	118.69	118.64	118.76	119.02	119.32	119.28
C(6)	155.08	154.84	154.95	155.16	155.29	155.12
C(8)	146.98	147.31	147.08	146.97	147.53	147.53
C(1′)	89.32	91.10	89.70	89.67	89.36	89.54
C(2′)	83.15	83.06	82.96	83.17	83.45	83.94
C(3′)	81.21	82.91	81.70	81.53	83.11	83.24
C(4′)	87.28	87.32	87.77	87.44	87.27	87.70
C(5′)	62.96	63.04	63.09	63.04	63.10	63.17
Uridine unit (I):						
C(2)	150.68	152.62	150.52	153.24	150.24	153.33
C(4)	163.98	162.80	163.84	163.26	164.14	163.58
C(5)	102.35	102.71	102.42	102.39	102.56	102.19
C(6)	141.92	152.20	142.15	151.34	142.91	151.09
CH_2–C(6)	–	62.40	–	62.39	–	62.34
C(1′)	93.71	91.46	93.90	91.23	95.37	91.11
C(2′)	84.84	84.91	84.44	84.15	84.56	84.87
C(3′)	81.21	81.41	81.07	80.93	81.66	81.98
C(4′)	88.78	89.22	88.17	89.48	87.44	88.41
C(5′)	68.12	67.98	68.42	69.04	33.46	33.92
C(6′)	139.94	143.11	140.10	140.49	137.23	138.14
C(7′)	118.30	117.17	118.00	117.07	117.62	116.88

[a]) Assignment based on HSQC spectrum.

suspension of **20** [2] (36 mg, 0.035 mmol), 5% Pd/$BaSO_4$ (18 mg), and quinoline (18 mg, 0.14 mmol) in MeOH (10 ml) was stirred under H_2 (1 bar) for 2 h at 25°. Filtration through *Celite*, evaporation, and FC ($CHCl_3$/MeOH 40:1) gave **21** (28 mg, 78%). White solid. R_f ($CHCl_3$/MeOH 20:1) 0.39. M.p. 132–134°. $[\alpha]_D^{25} = -19.2$ ($c = 1.0$, $CHCl_3$). UV ($CHCl_3$): 263 (13300), 301 (10500). IR ($CHCl_3$): 3412*w* (br.), 3186*w* (br.), 3029*m*, 2944*m*, 2866*m*, 1700*s*, 1635*m*, 1448*m*, 1428*m*, 1384*m*, 1264*m*, 1089*s*, 879*m*, 840*m*. ^{1}H-NMR (300 MHz, $CDCl_3$): see *Table 10*; additionally, 7.72–7.66 (*m*, 4 arom. H); 7.51–7.38 (*m*, 6 arom. H); 1.58, 1.54, 1.38 (6 H) (3*s*, 2 Me_2C); 1.10 (*s*, Me_3C); 1.00–0.89 (br. *s*, $(Me_2CH)_3Si$). ^{13}C-NMR (75 MHz, $CDCl_3$): see *Table 11*; additionally, 135.42 (*d*, 4 C); 131.83 (*s*, 2 C); 130.19 (*d*, 2 C); 127.94 (*d*, 2 C); 127.90 (*d*, 2 C); 114.26, 113.59 (2*s*, 2 Me_2C); 27.40, 27.28, 25.53, 25.42 (4*q*, 2 Me_2C); 26.68 (*q*, Me_3C); 19.33 (*s*, Me_3C); 17.93, 17.90 (2*q*, $(Me_2CH)_3Si$); 11.90 (*d*, $(Me_2CH)_3Si$). HR-MALDI-MS: 1062.482 ($[M+Na]^+$, $C_{53}H_{73}N_7NaO_{11}Si_2^+$; calc. 1062.480).

2′,3′-O-*Isopropylidene*-5′-O-*(triisopropylsilyl)adenosin-8-yl-(8→7′*-C*)-(6′*Z*)-1-(6,7-dideoxy-2,3*-O-*isopropylidene-α*-L-talo-*hept*-6-*enofuranosyl]uracil* (**23**). A suspension of **22** [2] (120 mg, 0.156 mmol), 5% Pd/$BaSO_4$ (60 mg), and quinoline (60 mg, 0.46 mmol) in MeOH (36 ml) was stirred under H_2 (1 bar) for 1 h at 25°. Filtration through *Celite*, evaporation, and FC ($CHCl_3$/MeOH 30:1) gave **23** (86 mg, 71%). White solid. R_f ($CHCl_3$/MeOH 20:1) 0.24. M.p. 156–158°. $[\alpha]_D^{25} = -66.8$ ($c = 2.0$, $CHCl_3$). UV ($CHCl_3$): 263 (9200), 301 (6850). IR ($CHCl_3$): 3413*w* (br.), 3200*w* (br.), 3017*s*, 2944*m*, 2867*w*, 1694*s*, 1635*m*, 1456*w*, 1384*m*, 1334*w*, 1270*m*, 1156*w*, 1085*m*, 931*w*, 881*w*, 809*w*. ^{1}H-NMR (300 MHz, $CDCl_3$): see *Table 10*; additionally, 1.60, 1.59, 1.39, 1.36 (4*s*, 2 Me_2C); 1.02–0.94 (*m*, $(Me_2CH)_3Si$). ^{13}C-NMR (75 MHz, $CDCl_3$):

see *Table 11*; additionally, 114.22, 114.10 (2*s*, 2 Me_2C); 27.44, 27.21, 25.53, 25.47 (4*q*, 2 *Me*$_2$C); 17.95 (*q*, (Me_2CH)$_3$Si); 11.93 (*d*, (Me_2*C*H)$_3$Si). HR-MALDI-MS: 794.3541 ([*M* + Na]$^+$, $C_{36}H_{53}N_7NaO_{10}Si^+$; calc. 794.3521). Anal. calc. for $C_{36}H_{53}N_7O_{10}Si$ (771.93): C 56.01, H 6.92, N 12.70; found: C 55.84, H 6.88, N 12.49.

2′,3′-O-*Isopropylidene-5′*-O-*(triisopropylsilyl)adenosin-8-yl-(8 → 7′*-C*)-(6′*Z*)-6-{[(*tert-*butyl)diphenylsilyloxy]methyl}-1-(6,7-dideoxy-2,3*-O-*isopropylidene-α*-L-talo-*hept*-6-*enofuranosyl)uracil* (**25**). A suspension of **24** [2] (39 mg, 0.038 mmol), 5% Pd/$BaSO_4$ (18 mg), and quinoline (18 mg, 0.14 mmol) in MeOH (10 ml) was stirred under H_2 (1 bar) for 2 h at 25°. Filtration through *Celite*, evaporation, and FC ($CHCl_3$/MeOH 30 : 1) gave **25** (29 mg, 74%). White solid. R_f ($CHCl_3$/MeOH 30 : 1) 0.21. M.p. 158–160°. $[\alpha]_D^{25} = +34.5$ (*c* = 1.0, $CHCl_3$). UV ($CHCl_3$): 264 (16900), 301 (11500). IR ($CHCl_3$): 3411*w* (br.), 3200*w* (br.), 3018*m*, 2944*m*, 2866*m*, 1698*s*, 1637*m*, 1462*m*, 1384*m*, 1337*w*, 1292*w*, 1223*s*, 1219*s*, 1211*s*, 1157*m*, 1096*s*, 1007*w*, 879*m*, 840*w*. ^{1}H-NMR (500 MHz, $CDCl_3$): see *Table 10*; additionally, 7.70–7.67 (*m*, 4 arom. H); 7.50–7.37 (*m*, 6 arom. H); 1.59, 1.51, 1.37, 1.33 (4*s*, 2 Me_2C); 1.07 (*s*, Me_3C); 1.02–0.96 (*m*, (Me_2CH)$_3$Si). ^{13}C-NMR (125 MHz, $CDCl_3$): see *Table 11*; additionally, 135.43 (*d*, 4 C); 131.79, 131.76 (2*s*); 130.23 (*d*, 2 C); 127.95 (*d*, 2 C); 127.90 (*d*, 2 C); 114.13, 114.06 (2*s*, 2 *Me*$_2$*C*); 27.56, 27.27, 25.67, 25.56 (4*q*, 2 *Me*$_2$C); 26.70 (*q*, *Me*$_3$C); 19.30 (*s*, Me_3*C*); 17.97 (*q*, (*Me*$_2$CH)$_3$Si); 11.97 (*d*, (Me_2*C*H)$_3$Si). HR-MALDI-MS: 1062.473 ([*M* + Na]$^+$, $C_{53}H_{73}N_7NaO_{11}Si_2^+$; calc. 1062.480). Anal. calc. for $C_{53}H_{73}N_7O_{11}Si_2$ (1040.36): C 61.38, H 6.89, N 9.44; found: C 61.40, H 7.08, N 9.32.

2′,3′-O-*Isopropylidene-5′*-O-*(triisopropylsilyl)adenosin-8-yl-(8 → 7′*-C*)-(6′*Z*)-1-(5,6,7-trideoxy-2,3*-O-*isopropylidene-β*-D-ribo-*hept*-6-*enofuranosyl)uracil* (**27**). A suspension of **26** [2] (80 mg, 0.106 mmol), 5% Pd/$BaSO_4$ (40 mg), and quinoline (40 mg, 0.31 mmol) in MeOH (20 ml) was stirred under H_2 (1 bar) for 20 min at 25°. Filtration through *Celite*, evaporation, and FC (AcOEt/cyclohexane 4 : 1) gave **27** (56 mg, 70%). White solid. R_f ($CHCl_3$/MeOH 20 : 1) 0.28. M.p. 121–123°. $[\alpha]_D^{25} = +15.9$ (*c* = 1.0, $CHCl_3$). UV ($CHCl_3$): 264 (15500), 296 (12200). IR ($CHCl_3$): 3491*w*, 3409*w* (br.), 3200*w* (br.), 2944*m*, 2867*m*, 1696*s*, 1636*s*, 1455*m*, 1384*m*, 1332*w*, 1270*m*, 1157*m*, 1090*s*, 882*m*, 807*w*. ^{1}H-NMR (300 MHz, $CDCl_3$): see *Table 10*; additionally, 1.60, 1.56, 1.40, 1.33 (4*s*, 2 Me_2C); 1.01–0.92 (br. *s*, (Me_2CH)$_3$Si). ^{13}C-NMR (75 MHz, $CDCl_3$): see *Table 11*; additionally, 114.47, 113.55 (2*s*, 2 *Me*$_2$*C*); 27.40, 27.10, 25.50, 25.33 (4*q*, 2 *Me*$_2$C); 17.78, 17.76 (2*q*, (*Me*$_2$CH)$_3$Si); 11.80 (*d*, (Me_2*C*H)$_3$Si). HR-MALDI-MS: 778.3540 ([*M* + Na]$^+$, $C_{36}H_{53}N_7NaO_9Si^+$; calc. 778.3572).

2′,3′-O-*Isopropylidene-5′*-O-*(triisopropylsilyl)adenosin-8-yl-(8 → 7′*-C*)-(6′*Z*)-6-{[(*tert-*butyl)diphenylsilyloxy]methyl}-1-(5,6,7-trideoxy-2,3*-O-*isopropylidene-β*-D-ribo-*hept*-6-*enofuranosyl)uracil* (**29**). A suspension of **28** [2] (63 mg, 0.062 mmol), 5% Pd/$BaSO_4$ (30 mg), and quinoline (30 mg, 0.23 mmol) in MeOH (18 ml) was stirred under H_2 (1 bar) for 30 min at 25°. Filtration through *Celite*, evaporation, and FC ($CHCl_3$/MeOH 80 : 1) gave **29** (30 mg, 48%). White solid. R_f ($CHCl_3$/MeOH 30 : 1) 0.20. M.p. 128–130°. $[\alpha]_D^{25} = +17.3$ (*c* = 1.0, $CHCl_3$). UV ($CHCl_3$): 265 (15300), 298 (11200). IR ($CHCl_3$): 3388*w* (br.), 3182*w* (br.), 2944*m*, 2866*m*, 1697*s*, 1637*s*, 1463*m*, 1428*w*, 1384*m*, 1334*w*, 1290*w*, 1219*s*, 1211*s*, 1157*m*, 1092*s*, 998*w*, 881*m*, 840*w*. ^{1}H-NMR (300 MHz, $CDCl_3$): see *Table 10*; additionally, 7.72–7.66 (*m*, 4 arom. H); 7.50–7.38 (*m*, 6 arom. H); 1.60, 1.52, 1.41, 1.32 (4*s*, 2 Me_2C); 1.09 (*s*, Me_3C); 0.99–0.92 (*m*, (Me_2CH)$_3$Si). ^{13}C-NMR (75 MHz, $CDCl_3$): see *Table 11*; additionally, 135.44 (*d*, 4 C); 131.83 (*s*, 2 C); 130.19 (*d*, 2 C); 127.94 (*d*, 2 C); 127.89 (*d*, 2 C); 113.80, 113.42 (2*s*, 2 *Me*$_2$*C*); 27.41, 27.30, 25.63, 25.52 (4*q*, 2 *Me*$_2$C); 26.68 (*q*, *Me*$_3$C); 19.32 (*s*, Me_3*C*); 17.94 (*q*, (*Me*$_2$CH)$_3$Si); 11.91 (*d*, (Me_2*C*H)$_3$Si). HR-MALDI-MS: 1046.476 ([*M* + Na]$^+$, $C_{53}H_{73}N_7NaO_{10}Si_2^+$; calc. 1046.486).

REFERENCES

[1] X. Zhang, B. Bernet, A. Vasella, *Helv. Chim. Acta* **2007**, *90*, 792.
[2] X. Zhang, B. Bernet, A. Vasella, *Helv. Chim. Acta* **2006**, *89*, 2861.
[3] J. S. Chen, R. B. Shirts, *J. Phys. Chem.* **1985**, *89*, 1643.
[4] B. Peterson, Ph.D. Thesis, University of California at Los Angeles, 1994.
[5] A. Kittaka, T. Asakura, T. Kuze, H. Tanaka, N. Yamada, K. T. Nakamura, T. Miyasaka, *J. Org. Chem.* **1999**, *64*, 7081.

[6] F. Mohamadi, N. G. J. Richards, W. C. Guida, R. Liskamp, C. Caufield, M. Lipton, G. Chang, T. Hendrickson, W. C. Still, *J. Comput. Chem.* **1990**, *11*, 440.
[7] P. Ballinger, F. A. Long, *J. Am. Chem. Soc.* **1960**, *82*, 795.
[8] Semichem, 'Program Ampac 8.16', Shawnee Mission, KS 66222.
[9] S. Eppacher, N. Solladié, A. Vasella, *Helv. Chim. Acta* **2004**, *87*, 2926.

Received January 9, 2007